8-2018

Experimental Investigation of Foam-Phase Change Material Interactions for Thermal Energy Storage

Prahlad Kulkarni
Purdue University

EXPERIMENTAL INVESTIGATION OF FOAM-PHASE CHANGE MATERIAL INTERACTIONS FOR THERMAL ENERGY STORAGE

by

Prahlad Kulkarni

Submitted to the Faculty of Purdue University
In Partial Fulfillment for the requirements for the degree of

Master of Science in Mechanical Engineering

School of Mechanical Engineering

West Lafayette, Indiana

Summer 2018

THE PURDUE UNIVERSITY GRADUATE SCHOOL
STATEMENT OF COMMITTEE APPROVAL

Dr Amy Marconnet, Chair

School of Mechanical Engineering

Dr John Howarter

School of Materials Engineering

Dr Liang Pan

School of Mechanical Engineering

Approved by

Dr Jay P Gore

Head of Departmental Graduate Program

To my Parents

Nanda Kulkarni and Uday Kulkarni

ACKNOWLEDGEMENTS

I would like to express my gratitude to my advisor Dr Amy Marconnet who mentored me throughout the course. This collaboration has been an invaluable learning curve. The experience has molded me into a responsible engineer who is ready to take on the challenges in industry. I appreciate her honest advice on the course selection and research projects. She made this thesis possible through immense patience through the editing phase. I would also thank Dr John Howarter and Dr Liang Pan for serving on the thesis committee.

I would like to extend my gratitude to the Ford Motor Company and Jody who is an engineer at Ford for providing us with this wonderful opportunity. I would also like to thank Collier Miers for guiding me in the project. Whenever I had any question/doubt, he was always ready to help since the beginning of my master's course, not just in my thesis project. I would also like to thank Prachi Kale who contributed to the paper, which I was fortunate enough to present at the prestigious ITHERM conference this year. Although my thesis project was not affiliated to the CTRC (Cooling Technologies Research Center), I would like to extend my gratitude to it as it laid down the foundation for my research thought in my first year. I was fortunate enough to get a chance to work on a project (Passive thermal management using phase change materials) under Yash Ganatra and got a chance to present it at the CTRC and develop positive relations with the industry members.

It has been a great ride here at Purdue for two years. I was exposed to high quality research and facilities, which I was not fortunate enough in my undergrad. It has laid down the foundations of my research thought, which would prove priceless in the future, wherever I go. The interaction with the students here paved the way for me to develop a different way of thinking towards the goals, which was hidden in me. The entire process of defining the project objectives, keeping up with the time line, evaluating the results and thesis writing has allowed me to learn and effectively apply my thought in research. At last, I would like to thank my parents for un-parallel support and motivation throughout the course.

TABLE OF CONTENTS

LIST OF FIGURES

ABSTRACT

Author: Kulkarni Prahlad, MSME
Institution: Purdue University
Degree Received: Summer 2018
Title: Experimental Investigation of Foam-Phase Change Material Interactions for Thermal Energy Storage
Committee Chair: Amy Marconnet

High-density electronics and avionics such as Insulated gate bipolar transistor (IJBTs) and transistors, as well as vehicles themselves, generate excess heat, which must be dissipated to prevent overheating and failure. Phase change materials (PCMs) both rapidly dissipate heat through melting and can store this useful thermal energy for future use. The effectiveness of PCMs is limited by low thermal conductivity, thus, high conductivity metal foams are often introduced to improve the thermal storage performance. In the first part of this thesis, the melting and solidification behavior of a phase change material in a single millimeter-scale cavity is investigated with high resolution infrared (IR) microscopy and compared to numerical models. In the second part of this thesis, the melting and solidification behavior of PCM embedded in commercially available metal foams is explored with high-resolution infrared microscopy.

The primary objective of the first experiment is to experimentally evaluate melting and solidification in small individual pockets of phase change material. In particular, we investigated phase change dynamics in cylindrical cavities of varying diameter. The melt/solidification front was tracked and radial temperature distribution curves were obtained to understand phase change in small pockets. This is a precursor to the study of phase change in foams with multiple pores.

In the second part, IR microscopy directly observes the impact of foams on the phase change process. Since this work concentrates on heat recovery, more attention is given to the solidification behavior than to the melting behavior. The interface between the foam and PCM is closely observed to understand the thermal interaction between the solid high thermal conductivity scaffold and the phase change material. The foams significantly reduce the solidification times by approximately a factor of 3 due to localization of phase change within the pores and the high effective thermal conductivity of the composite which aids in efficient heat spreading. Decreasing the pore size (increasing the pores per inch within the available range) has little effect on the phase change time.

Ultimately, this work provides new insight into the phase change dynamics assisted by high conductivity metal foams for better heat spreading which ultimately will enable the design of better, more efficient thermal storage systems with improved phase change response

CHAPTER 1. INTRODUCTION

Today, fossil fuels serve for the majority of all modern energy needs. Massive power plants burn fossil fuels such as coal, natural gas, and oil to produce electric power. Since our energy needs vary from day to day and within the day, the system needs to be flexible enough to provide energy at the right time. One advantage of fossil fuels lies in their high calorific content meaning they can produce high energy density by burning a reasonable amount [1]. Fossil fuels have changed our daily lives, but are not the answer in the long run due to their non-renewable nature [1]. It is estimated that our oil reserves are going to run out in ~30 years, gas in ~40 years, and coal could last until about the 2080's [2]. However, a government study [3] reveals that the world energy demand is increasing and will rise by 28% by 2040. Thus, even as fossil fuel reserves are decreasing, the demand for energy is increasing at an alarming rate. But, the non-renewable nature of fossil fuels and their impact on the environment is urging the world to move to renewable sources of energy such as hydro, wind, and solar energy.

However, due to climatic inconsistencies, storage of energy is becoming more and more important [1]. The effectiveness of the storage system depends on the capacity of storage, response time, and the operating temperature range. A good storage system enables the user to retrieve the stored energy in desired quantities and at the desired time and it can quickly restore the lost energy in minimum time possible. Combining the use of renewables and effective storage systems can help in battling climate change [3].

Energy storage systems can come in various forms depending upon the type of energy being stored. Dams, batteries, flywheels, and capacitors are examples of energy storage systems leveraging potential, electrochemical, mechanical, and electrical methods. This work focusses on thermal energy storage, which has numerous applications such as sterling engine, thermal power plants, air conditioning, heaters, and even in clothing. There are two types of thermal energy storage: 1) *sensible heat storage*, which makes use of the heat capacity of the system and 2) *latent heat storage*, which makes use of the phase transition phenomenon of the system. Latent heat storage systems can store much more thermal energy per a given volume due to high latent heat of phase change compared to the lower specific heat value.

Additionally, there have been many attempts to recover thermal energy for useful purposes. For example, the sterling engine is one of the most popular ways to recover thermal energy [5]. It is a heat engine, which converts heat energy into mechanical power. However, this method has many drawbacks. The efficiency is generally between 15 and 30 % [5], which means most of the heat energy is not used effectively. The dynamic parts add losses due to friction. Thus, a more compact, highly efficient way to storage/recover heat energy is required. One of the ways to do this is through phase change materials (PCMs), leveraging their high latent heat for effective storage. Such systems store thermal energy and release it when required for instance, storing solar energy or waste heat during the day to provide heat at night. This significantly contributes to energy recovery and could reduce the cost of power. The heat recovery/thermal storage capability of PCMs can be used in many ways such as in heat exchangers for automotive waste heat recovery [7], in the walls of buildings in thermal management and occupant comfort [8], in solar thermal energy storage [9], for cooling of clothes [10], and in military and space applications for equipment cooling [11].

One of the major drawbacks of phase change materials is their low thermal conductivity. Thus, it takes a long time for the heat to spread throughout the volume of PCM, thereby reducing the phase change response time. Embedding the PCM in high thermal conductivity foams enhances the heat spreading throughout the volume of the storage medium improving responsiveness, but at the drawback of reducing the volumetric storage capability with the fully solid foam scaffold.

1.1 Overview of this Thesis

This thesis investigates phase change materials as a mode to store/recover thermal energy, in particular focusing on the interaction of the phase change material with high thermal conductivity support structures to improve performance.

- Chapter 1 provided a brief overview of phase change materials and their applications.
- Chapter 2 reviews phase change materials, the need for effective heat spreading within them, and thermal storage using phase change materials.
- Chapter 3 experimentally evaluates the evolution of the temperature profile during melting in a cylindrical geometry and compares the data to computational models of the phase change process.
- Chapter 4 introduces heat spreading using foams with experimental evaluation of the

melting and solidification process.

- Chapter 5 concludes the project and provides future recommendations.

CHAPTER 2. BACKGROUND ON PHASE CHANGE MATERIALS

Phase change materials (PCMs) have become a key component in thermal storage in the recent years due to their high latent heat values. This chapter introduces the thermodynamics of phase change materials and some common ways to enhance their phase change response due to their poor thermal conductivity.

2.1 Phase Change Dynamics

For a pure material, as heat is applied to a solid, it heats up until the phase transition point. During melting, the temperature is approximately constant as the sample undergoes a state change (in this case, from solid to liquid), after which the temperature rises again due to sensible heating as shown in Figure 2.1. The time required for phase change depends on the amount of phase change material, rate of heating/cooling, and the specific latent storage capacity. The temperature profile during cooling is simply the reverse of the heating diagram, although undercooling can depress the solidification temperature compared to the melting temperature.

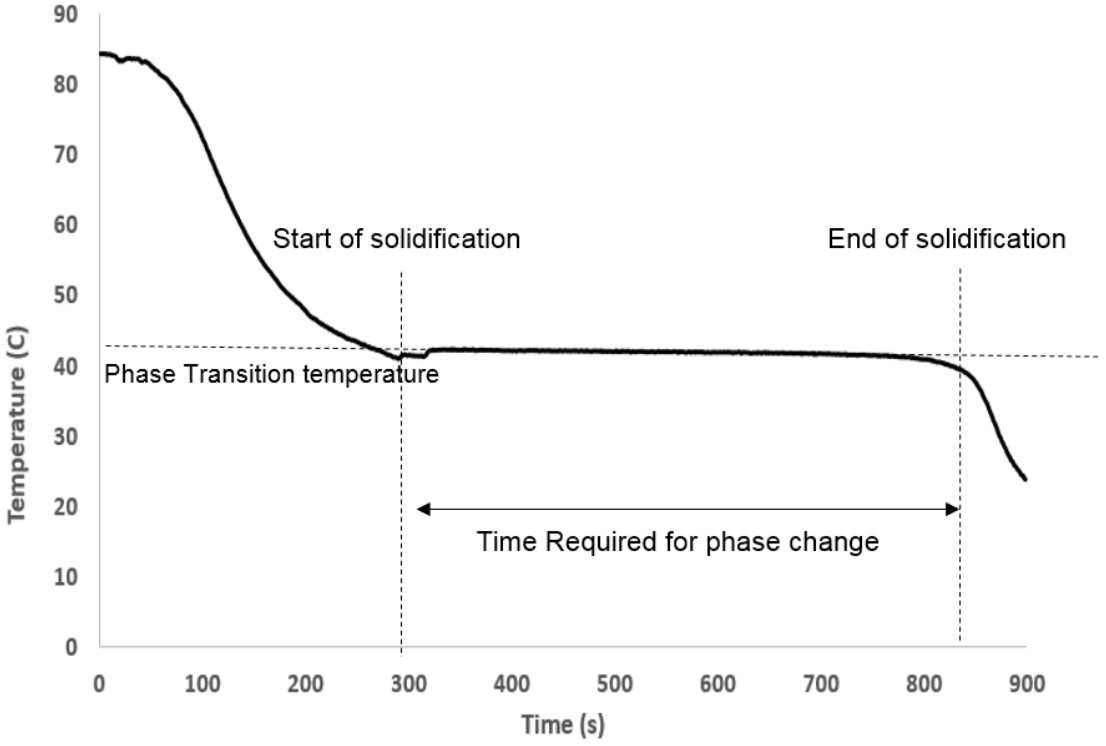

Figure 2.1 Plateau at the melting temperature indicative of the phase change process

2.2 Classification of Phase Change Materials

Phase change materials can be classified into categories based on composition including organic, inorganic, or eutectic compositions. Organic PCMs typically possess good phase change properties such as latent heat, good chemical compatibility, and they generally do not suffer from undercooling (which reduces the phase change response during solidification). Various requirements and criteria must be evaluated to select an appropriate phase change material for a particular application. For example, for most systems, a good phase change material will have a high latent storage capacity, a high density, and a reasonably good thermal conductivity [12].

2.3 Methods to Improve Heat Spreading

Phase change materials generally suffer from low thermal conductivity [13], which hinders the phase change response and efficiency of the thermal storage system. Integrating heat spreaders to form composite PCMs can increase the effective thermal conductivity. Heat spreaders are often made of high thermal conductivity metals [15] or carbon-based materials [18]. There are various kinds of heat spreaders such as fins [16, 17], and flakes [18, 19] foams [20, 21].

2.3.1 Heat Spreading with Fins

Metal fins in various configurations (e.g., longitudinal, radial, or pin fins) can be embedded in PCM to conduct the heat [16], [17], For example, Arshad et al. [16] investigated a pin fin-PCM composite for electronic thermal management. The 72 pin fins vastly increased the surface area for heat exchange between the metal and the PCM. The onset of phase change occurs quicker and time taken for phase change is reduced compared to the case without the fins. Similar to solid fins, including heat pipes can effectively transfer heat along the length of the sample. For example, Yang et al. [17] used a finned heat pipe in the design of a PCM based heat sink for high thermal power “shock” applications of $10 W/cm^2$. The design helped prolong the working duration of the sink by a factor of 1.4 to 2.5 compared to a similar heat sink without the heat spreader.

2.3.2 Heat Spreading with Particulate Inclusions

In a second approach, particles with higher thermal conductivity are mixed into the PCM to enhance the overall effective thermal conductivity of the composite. The direction of orientation

of the particles play a vital role with the effective thermal conductivity enhanced in the direction of orientation [19]. In recent work, few layer graphene (FLG) flakes are effective at increasing the thermal conductivity of the PCMs by up to two orders of magnitude [19]. Limitations of this approach include settling or sedimentation of the particles during cycling and the lack of a contiguous scaffold of high conductivity material through the material at low density of the particles.

2.3.3 Heat Spreading with Foams

Foams overcome many of the challenges of the particular composites and spread heat effectively due to their interlinked and continuous solid structure. Within the foams, the PCM is split into small chunks whose boundaries are defined by the foam pores. Thus, this increases the overall surface area for heat transfer into the PCM and lowers the response time of the phase change medium.

Most commercially available metal (e.g., copper, aluminum) foams consist of approximately hexagonal structures and are characterized by a pore density in pores per inch (PPI) and porosity (volume fraction of voids within the foam). The pores density varies from ~5 pores per inch (PPI) to ~100 PPI [20]. Higher PPI indicate smaller the pores and smaller distance that heat must travel for the foam to melt. The porosity directly effects effective thermal conductivity. Lower porosities indicate more solid volume and higher effective thermal conductivity (at the sacrifice of the latent heat).

Many researchers have studied the impact of foams on PCMs. For example, Mustaffar et al. [21], investigated the transient behavior of an aluminum foam-PCM system and found that the foam enhanced the effective thermal conductivity by a factor of 22 to 10.49 W/m/K. Ji et al. [22] investigated graphite foams finding an 18-fold enhancement in thermal conductivity. These works demonstrate the promise of foams for enhancing thermal conductivity. Although there is abundant literature available on heat spreading using foams, there is little information on the thermal interaction between the foam and the PCM and heat spreading can be limited by the interaction at the interface. Thus, the current thesis investigates how the PCM and the metal foam interact at the interface in terms of temperature distribution, which can shed more light on heat flow between the two.

2.4 Conclusions

This chapter introduced the concept of thermal storage using PCMs including integrating PCMs into thermal energy storage systems. Heat spreaders are required to enhance the phase change response of the PCMs due to their poor thermal conductivity. Several researchers have demonstrated that PCMs can be integrated with high conductivity heat spreaders, which aids in efficiency of the thermal storage system. But more work is required on the quantification of the thermal interaction between the foam and PCM as this information can be used to custom design thermal storage systems depending on the application. This can be carried out through measurements of the temperature distribution across the foam-PCM interface and the interfacial conductance.

CHAPTER 3. COMBINED EXPERIMENTAL-NUMERICAL INVESTIGATION OF METAL -PCM INTERACTIONS FOR PHASE CHANGE THERMAL ENERGY STORAGE

This section partially reproduced from P. Kulkarni, P. Kale, C. Miers, and A. Marconnet, "Combined Experimental-Numerical Investigation of Metal -PCM Interactions for Phase Change Thermal Energy Storage", 2018 Intersociety Conference on Thermal and Thermomechanical Phenomena in Electronic Systems (ITHERM), San Diego, CA, 2018.

3.1. Introduction

Phase change materials (PCMs) have gained tremendous momentum over the last decade due to their ability to store thermal energy and passively regulate temperature. There are numerous applications of PCMs such as storage of heat in automobiles, cooling and temperature control of electronics, and military and space-based technology [23], as well as extending solar power plants to 24-hour cycles [24]. In electronics cooling, phase change materials can delay the time taken to reach a thermal management cut-off temperature of the chip delaying the onset of thermal throttling that impedes the performance of the processor to maintain safe operating temperatures [25]. Further, PCMs are used in military applications such as cooling of gun barrels and cooling of jackets of soldiers [26]. They are used as thermal capacitor in space systems as their performance fairly matches with that on terrestrial systems [23]. In solar power plants, and in heat exchangers in general [23], tubes within the heat exchanger are filled with PCMs and the fluid flow dictates the storage/release of heat.

Most phase change materials used in these applications have high latent heat, but poor thermal conductivity [26]. Thus, to enhance thermal conductivity the PCM, it is often integrated with metallic heat spreaders such as foams [27] and fins [28]. While these systems have been experimentally demonstrated to improve performance, there is little work on the thermal interaction between the phase change component and the solid heat spreader. To probe the physics of this system, here, we examine the melting and solidification behavior of a cylindrical plug of

phase change material in a high conductivity aluminum block. The temperature and phase change fronts are measured experimentally using a high-resolution infrared microscope. These results are compared with numerical simulations of the phase change process.

Phase change materials are efficient at storing thermal energy due to their high latent heat values. However, they suffer because of low thermal conductivity and low thermal diffusivity. To make them more effective, they are often encapsulated or integrated with high conductivity foams or filler materials. As an example, Hawlader et al. [29] investigated encapsulated PCMs in packed beds demonstrating high latent storage and energy release capacity. Sun et al. [30] tracked the melt-front within a cylinder of paraffin PCM based slurry with silica alumina microspheres to enhance heat spreading. For lower particle loading (5%), heat transfer is dominated by convection and this transition to conduction as the loading increases (to 50%). Dhukan et al [27] investigated the impact of using aluminum foam to enhance the effective thermal conductivity for better phase change response. It was concluded that the foam inclusion cut down the solidification time by 42% and melting time by 15.3%. The maximum temperature while heating was also cut-down by 11%.

Many works have already evaluated phase change in cylinders finding that convection can play a dominant role depending on geometry, orientation, and heating conditions. For example, Hlimi et al. [31] investigated the melting of PCMs in horizontal cylinders tracking the liquid fraction and the melt-front as the PCM melts. The samples melted faster with increasing Rayleigh number due to the convection dominated heat transfer. Dhaidan et al. [32], Jones et al. [33], and Shmueli et al. [34] investigated melting and solidification of PCM in vertical cylinders finding that the impact of convection depends on which walls are heated and the degree of sub cooling or superheat. Wu and Lacroix [35] showed that highest heat transfer rates are observed at the bottom of a uniformly heated cylinder where natural convection occurs. Muhammad et al. [36] validated a commercially available CFD code for melting and solidification in vertical cylinders through comparison to previous experimental results including melt fraction with an error of 7.5%. Sparrow and Broadbent [37] specifically investigated the role of fluid motion by natural convection on rate of melting and energy storage. With no sub-cooling, the energy transfer associated with melting was found to be 50% greater than pure conduction model due to convection effects.

The melting rate was found to decrease as the PCM melted due to reduced surface area for

heat transfer. Here we focus on small vertically oriented cylinders to minimize the effect of natural convection on the system. While much literature focused on convection effects and overall thermal performance, the goal of this paper is to understand the physics of solidification in the cylindrical system in part to validate models of phase change.

3.2. Experimental Procedure

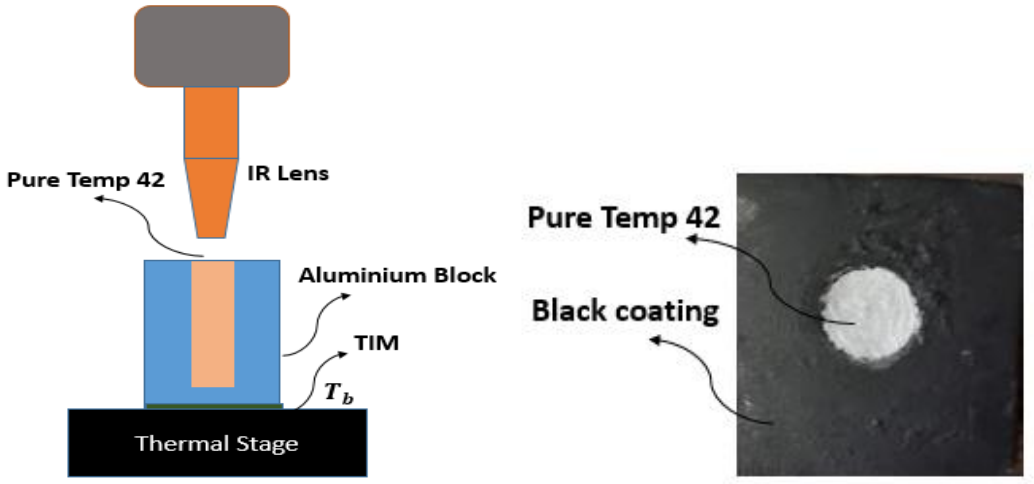

Figure 3.1 (left) Schematic of the experimental set-up consisting of an aluminum block with a high aspect ratio cylindrical hole filled with PCM. The thermal stage controls the temperature of the aluminum block. The infrared microscope observes from the top. (right) Top view image of the prepared sample including the aluminum region coated with a high emissivity black coating and the phase change material in the 1 cm diameter cylindrical pocket

This work measures the melting and solidification behavior of a phase change material embedded in an aluminum block (7 x 3.5 X 5 cm). A high aspect ratio [H/d=4] hole in the aluminum is filled with PCM and approximates a 1-D radial system at the top surface where the microscope can observe the temperature profile (see Figure 3.1). While it is challenging to fully observe the temperature gradients in phase change systems using conventional thermal metrology tools like thermocouples, our high-resolution infrared microscope (Infrascope, Quantum Focus Instruments Corporation) enables measurement of the temperature profiles with 1.8 µm spatial resolution throughout the melted and solid regions. Extensive calibrations have been done to ensure the accuracy of the temperature data for the PCM in both the molten and solid states. The aluminum block is placed on a thermoelectric controlled thermal stage and the temperature of the

thermal stage is controlled and measured during the experiment. While a step change in temperature would be ideal, the thermal mass and limits on the cooling and heating power of the stage lead to a ramp like increase or decrease in the temperature of the aluminum block. The Biot number quantifies the uniformness of temperature within any body. If the value is less than unity, then the temperature is more or less uniform spatially. The value for this system was computed to be around 0.01. Thus, we can conclude that the block temperature is relatively uniform. This was also verified using COMSOL models.

3.3. Computational Model

In parallel with experiments, we model the system in COMSOL Multiphysics ® using the apparent heat capacity method that is built into the commercial code. The apparent heat capacity method inflates the heat capacity in the temperature range around the melting point to model the phase change process. Here we use a melting point of 42^{o}C with a phase transition range of 5^{o}C. The material properties for the PCM are taken from [38]. The system is modeled in 2-D. The temperature at the bottom surface of the aluminum block is set as that measured in experiments, while all other exposed surfaces experience convective losses at 5 W m^{-2} K^{-1} to ambient conditions (19°C). Figure 3.2 illustrates the computational model.

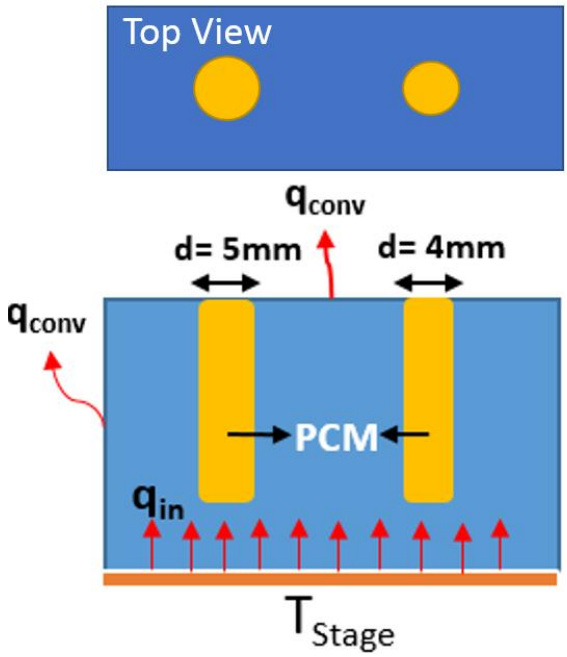

Figure 3.2 The model, which was used in COMSOL to simulate the experiment. The yellow regions indicate PCM with red arrows indicating the direction of heat transfer

3.4. Results and Discussion

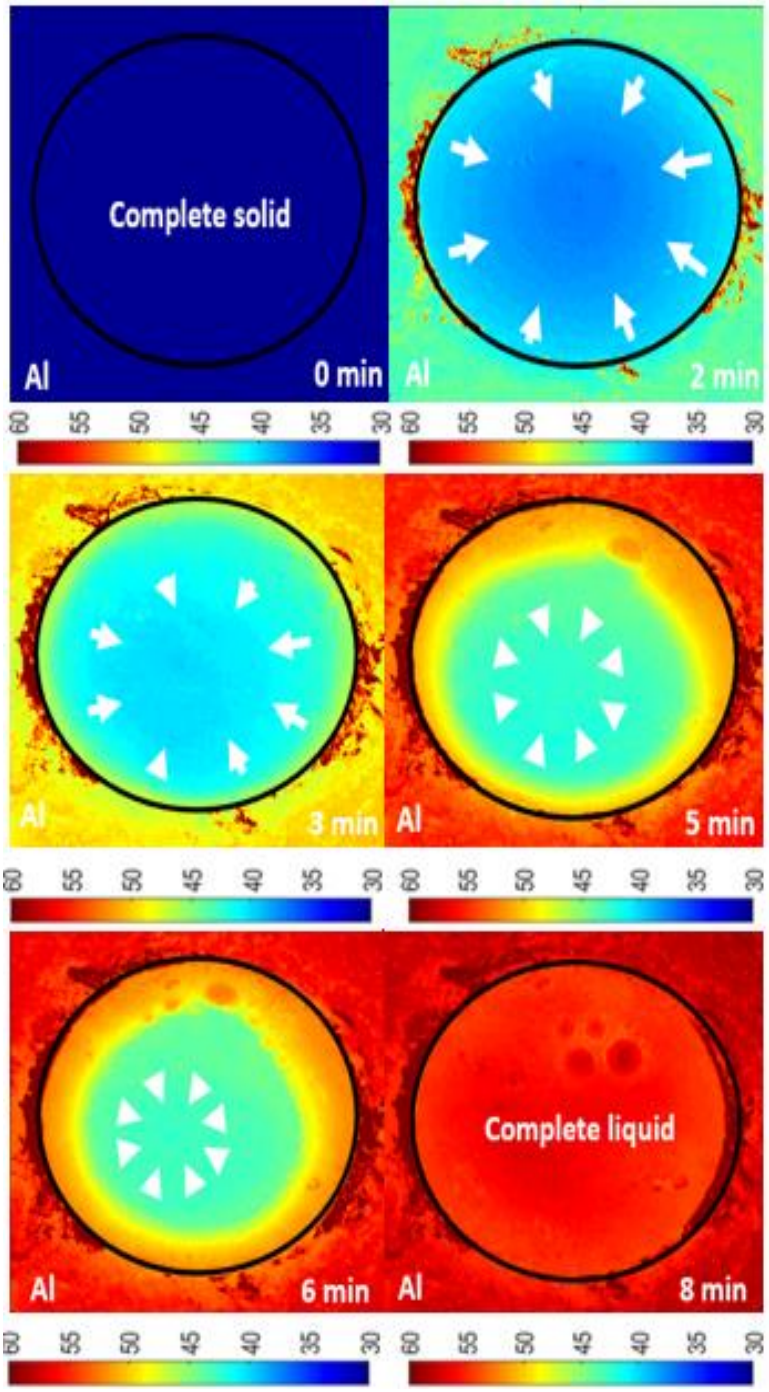

Figure 3.3 Left: Selected thermal images during melting. The cavity is 5 mm in diameter with the edges highlighted by the black line. Arrows roughly indicate the edge of melt front and the direction of propagation. Note that once the solid plug is fully released from the side and bottom, the solid region moves off center due to convection effects. Color bars indicate temperature in degrees Celsius

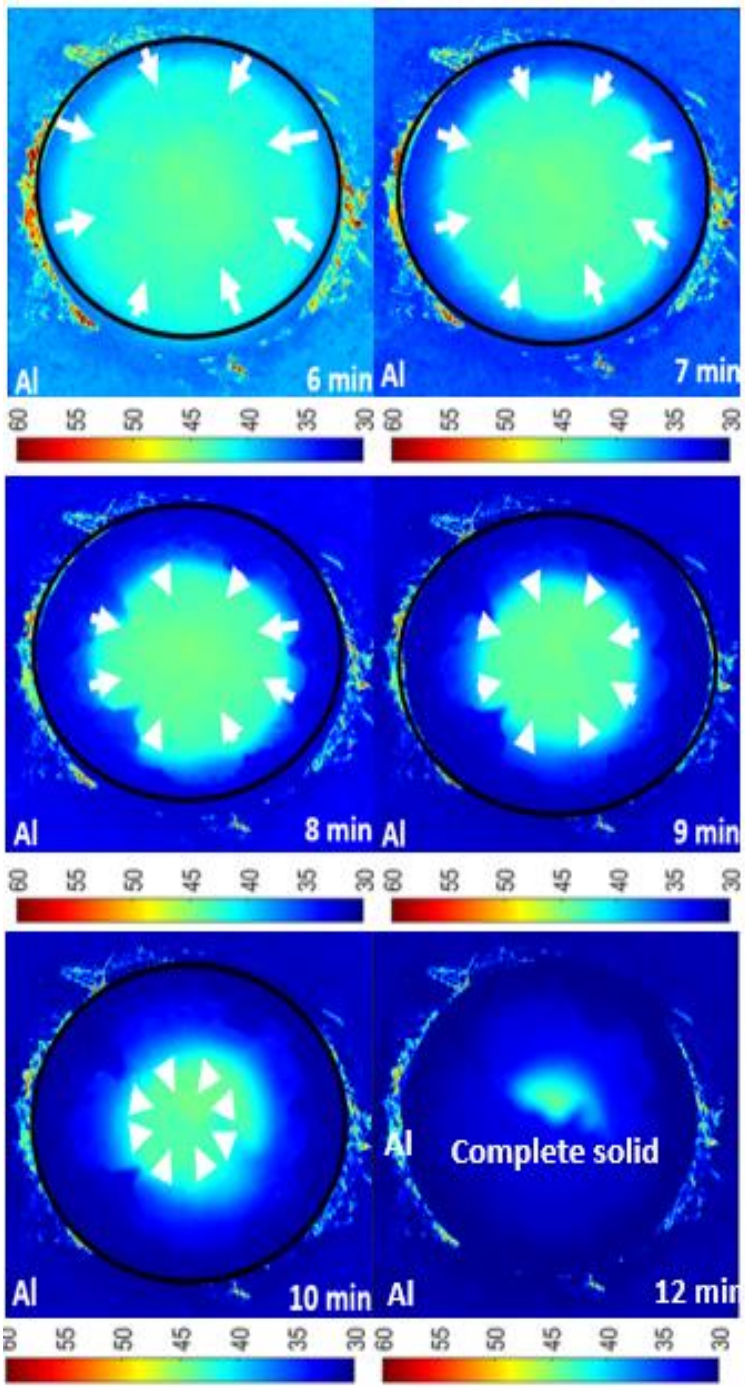

Figure 3.4 Selected thermal images during solidification. The black line 5 mm in diameter with the edges highlights the cavity. Arrows roughly indicate the edge of solidification front and the direction of propagation. Color bars indicate temperature in degrees Celsius

Temperatures during melting and solidification are captured using the IR camera at several time intervals. The solid-liquid interface location was visually tracked as shown in Figures 3.3 (melting) and 3.4 (solidification). The ‘mushy zone’, which is in between solid and liquid phases, are observed in some images. Melting takes less time compared to solidification due to limitations of the thermal stage. Figure 3.5 show the edge and center temperatures over time. The 2D temperatures maps are averaged in concentric cylinders using MATLAB. The temperature as a function of radial location are plotted in the Figures 3.6 and 3.7, while the location of the melting/solidification front over time is illustrated in Figure 3.8.

3.4.1 Sample Center and Edge Temperatures.

The stage temperature was ramped from 30°C to 60°C for melting and ramped back to 30°C for solidification. Figure 3.5(a) shows the variation of PCM edge temperature and Figure 3.5(b) shows the center temperature with time during these processes. We can observe that during melting, the center temperature increases then saturates at the melting temperautre for several minutes. But after the materially fully changes phase, super heating of liquid occurs and the temperature rises quite rapidly. This is due to the fact all the heat generated by the thermal stage is used for sensible heating of the liquid PCM. A similar but opposite trend can be observed during solidification. The temperature decreases steadily up to the phase change point where it remains for several minutes until again decreases steadily after the sample has fully undergone phase change.

The below figures are the matlab images of melting and solidification of PCM. We can observe that during melting, the PCM block (cylinder) goes off center due to convection effects and is not visible after 6 min as it gets submerged inside the liquid due to reuction in its height below the full height of the block in which it is placed.

The cavity edge temperature, which is taken as the interface between PCM and aluminum, increases at a steady rate then tends to saturate at around 57°C -58 °C which is very close to the stage set temperature at the base (i.e., the aluminum is fairly isothermal). During solidification, temperature decreases at a steady state then tends to saturate again at the set stage temperature of 30°C, but this takes longer due to the limited cooling power of the thermal stage. The difference between the center and edge temperature increases with time for both melting and solidification.

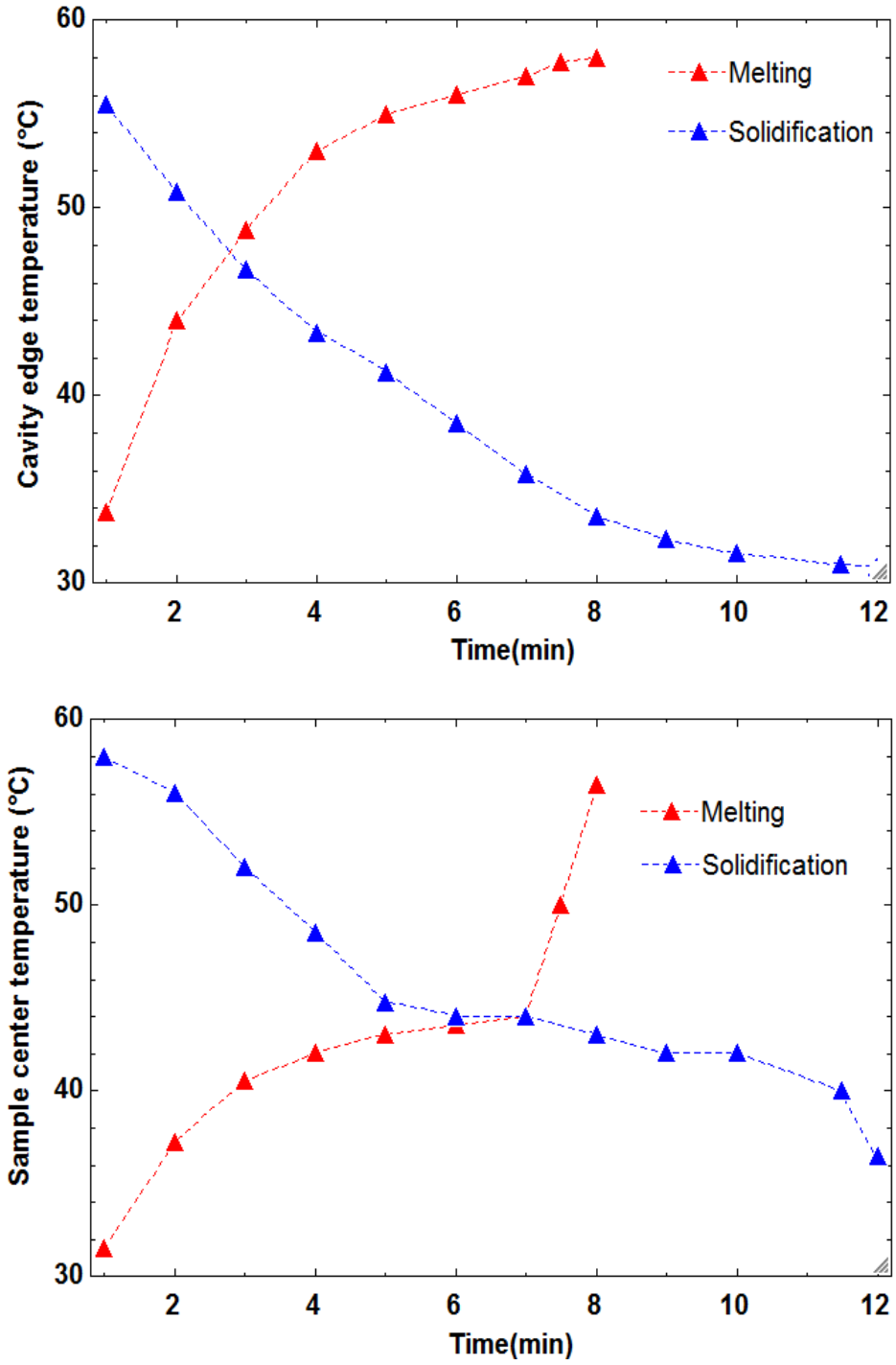

Figure 3.5 (a) Sample edge temperature and (b) cavity center temperature temperatures. Note that cooling the block from 60°C to 30°C (during solidification) is slower than heating from 30°C to 60°C (during melting) because of limitations in cooling power of the thermal stage. Thus, the solidification process takes longer than the melting process, because the heater power is greater than the cooling power. Plateaus in the temperature history during melting and solidification are observed in the temperature history of the sample during the melting and solidification processes

3.4.2 Radial Temperature Distribution.

The 2D temperature images obtained from IR are averaged within concentric circles using a MATLAB code to provide a 1D representation of the temperature as a function of position at a few snapshots in time shown in Figures 3.6 and 3.7. The computational results from COMSOL differ somewhat from experimental data. Ultimately, more calibration of the COMSOL models will be required including better estimation of material properties and boundary conditions. Note that the magnitude of the temperature gradient near the edges of the cavity are greater during melting than for solidification because thermal stage power is greater during heating than during cooling. Figure 9 confirms that melting occurs much faster compared to solidification.

During solidification, the temperatures drops faster in the experiment compared to COMSOL results. This could be due to convection effects within the cylindrical cavity observed in the real case, which is not considered in the computational model. Note that the boundary conditions in the model were based on the experimentally observed heating and cooling ramp rates for the thermal stage: 100 s was used as the ramp up time from 30^{o}C to 60^{o}C during melting simulations and 500 s was used as the ramp down time from 60^{o}C to 30^{o}C during solidification.

Figure 16 shows how the solid-liquid interface moves during melting and solidification. We can observe that during melting the experiment and simulations do not agree after 3min. This could be because as the sample melts, the solid portion starts to decrease in its height, as the material is liquified at the bottom, thus the IR camera is blinded by this after 3 min as it can now only see the liquid surface on top.

The comparison is much more reasonable during solidification as can be observed throughout the length of the experiment. However, there is a small deviation observed due to the mismatch in the thermal stage-cooling rate between the measured and actual values. We can generally observe that solidification takes more time compared to melting as it is a natural phenomenon.

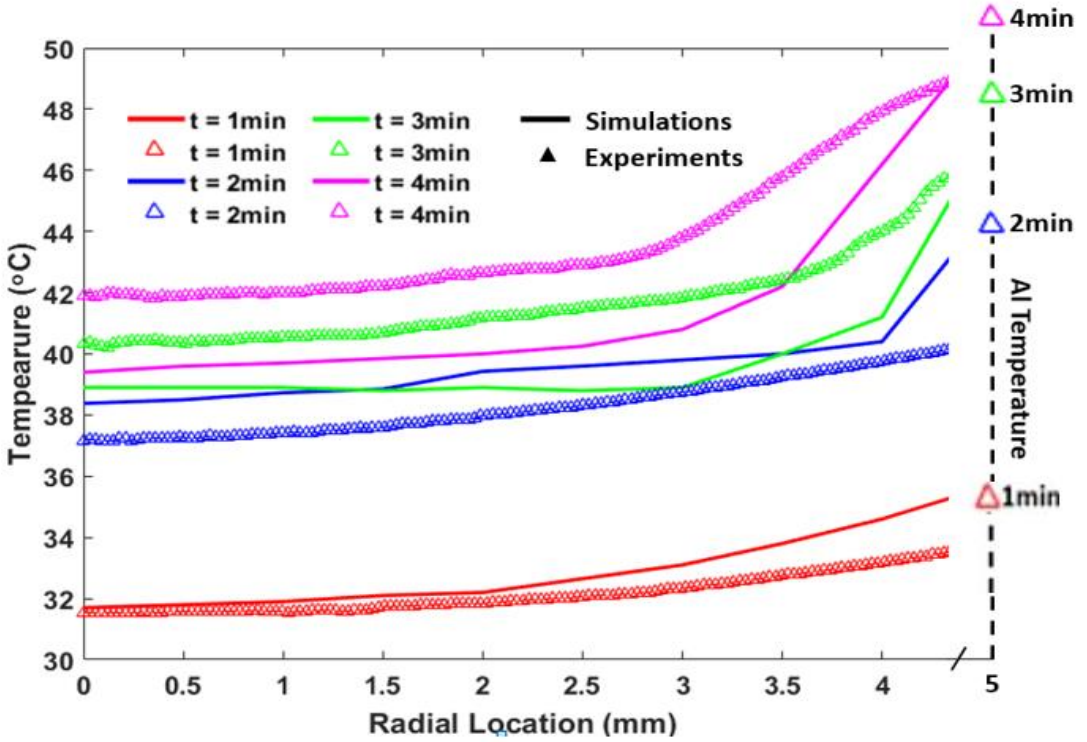

Figure 3.6 Radial Temperature distribution during melting

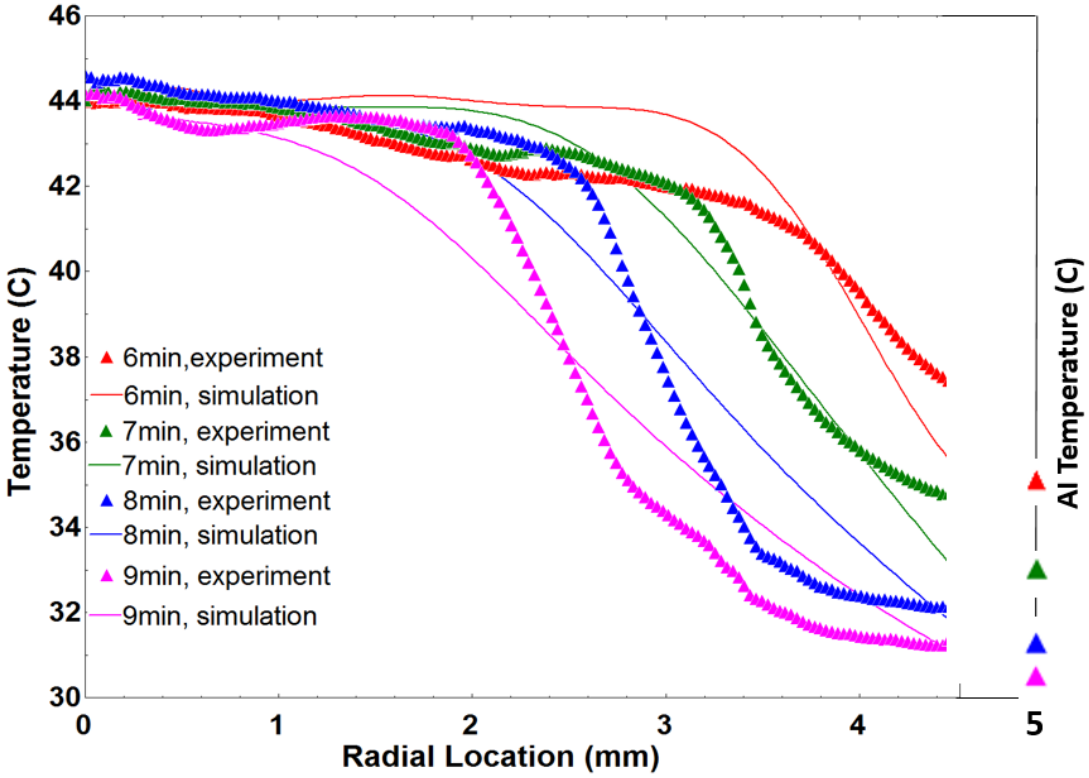

Figure 3.7 Radial Temperature Distribution during solidification

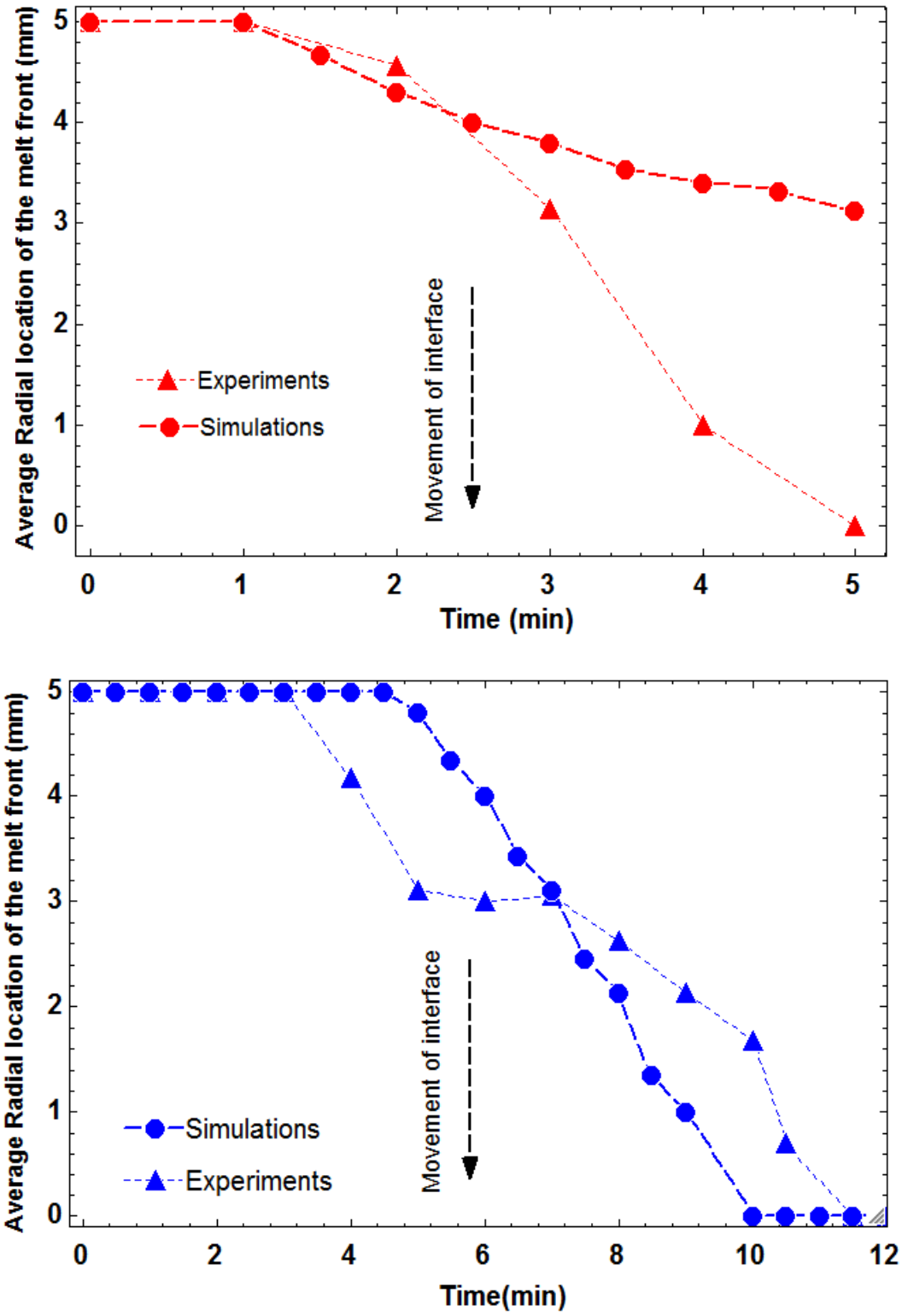

Figure 3.8 Interface location during melting (top) and solidification (bottom) from the experiments (▲) and simulations (●)

3.4.3 Hole Size Comparison

The phase change response of the 4mm and the 5mm cavity was compared. This included the comparison plot of the interface location (Figure 3.9). It can be observed that the solidification of the 5mm cavity kicks off faster but is overtaken by the 4mm cavity. The 4mm cavity takes 2min less time to solidify. It can also be observed that the center temperature of 5mm cavity is slightly higher compared to the 4mm cavity. However, the edge temperature appears to be similar. From the plots, we can conclude that the mechanism of phase change is similar for a cavity of any diameter.

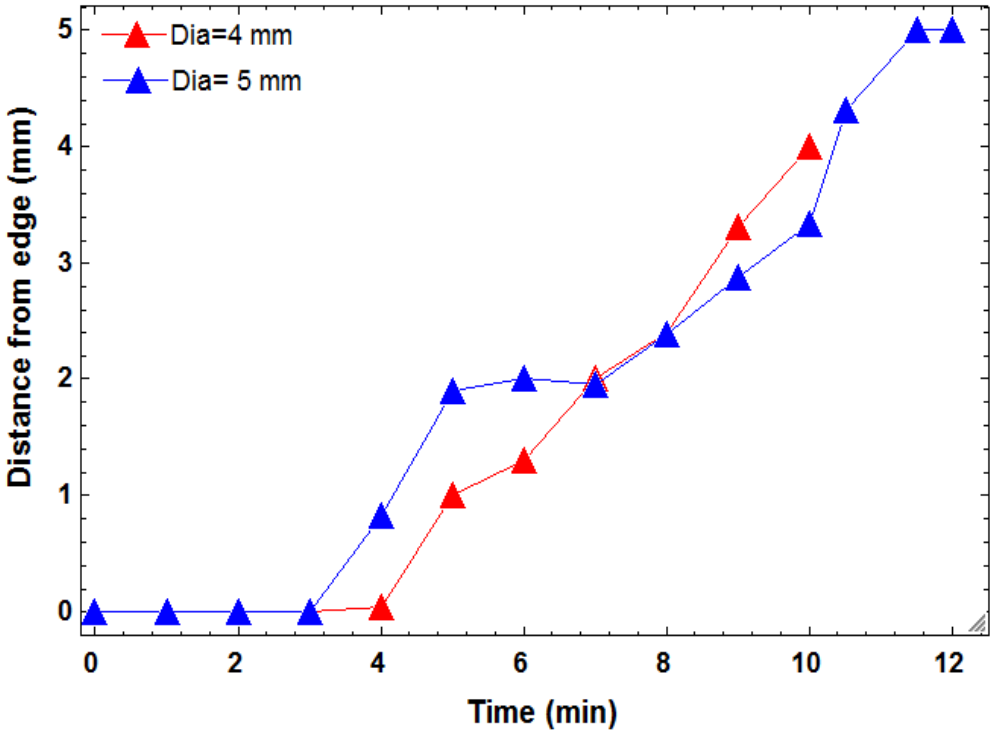

Figure 3.9 The melt-front (tracked by measuring the location of the interface from cavity edge) as a function of time. The average slope for the 4-mm diameter hole is greater meaning it solidifies faster

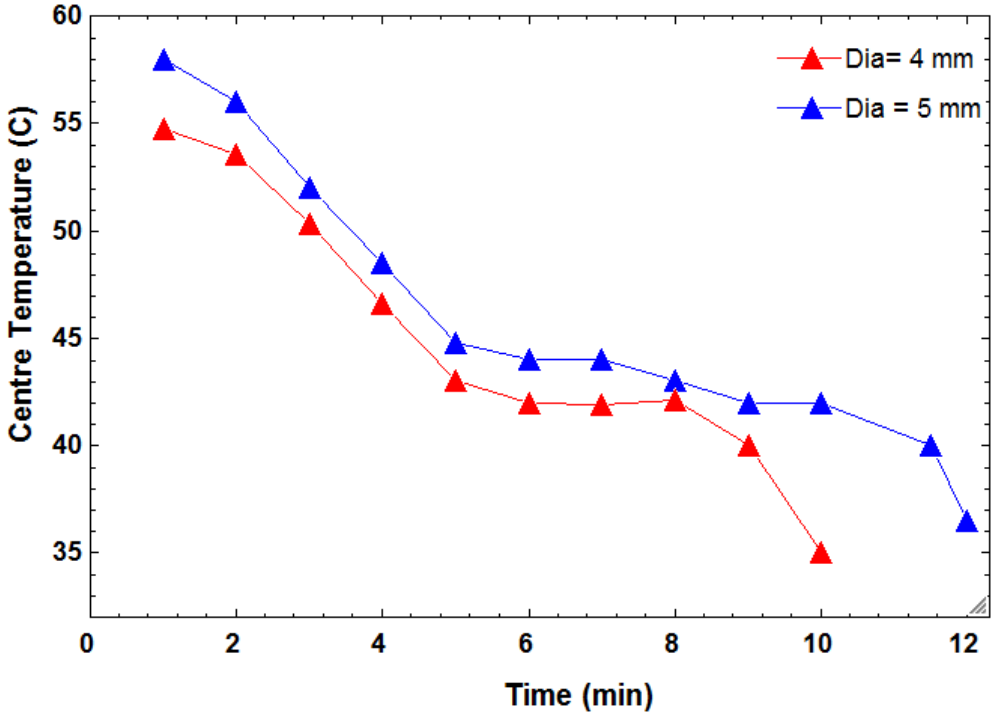

Figure 3.10 Comparison of center temperature of the two holes during solidification. The 4mm diameter hole is cooler throughout the process than the 5mm diameter hole

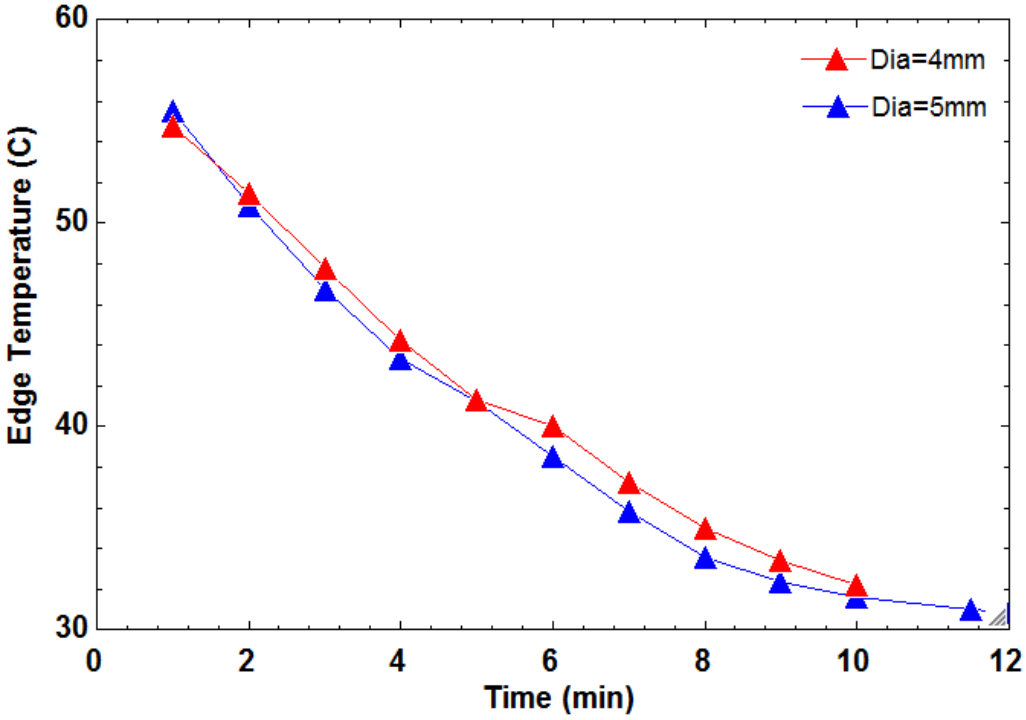

Figure 3.11 Comparison of the edge temperature of the two holes

3.5. Conclusions

In this study, the melting and solidification behavior is investigated for a commercially available phase change material. The spatial and temporally varying temperature history elucidates key phenomenon. In the future, the analysis will be extended to cavities of different diameter to see how the size impacts the phase change process. The experimental data will enable comparison with more advanced phase change simulations. Specifically, a fully 3D computational analysis will be carried out to better quantify the effects of fluid convection on melt characteristics near the surface. We plan to further evaluate the contact resistance between PCM and aluminum, which is essential for future computational models involving composite PCMs. Finally, experiments with varying stage temperatures will illustrate the impact of phase varying super heat.

CHAPTER 4. INVESTIGATION OF HEAT SPREADING USING FOAMS

Phase change materials are effective at storing thermal energy, but their low thermal conductivity impedes heat transfer, thereby increasing the phase change response time, which is not ideal for a good thermal storage system. Here, the effective thermal conductivity is increased by introducing high conductivity metal foams. This chapter details experimental efforts to understand the melting and solidification behavior of the composite systems, and, in particular, the interaction at the interface between the solid foam scaffold and the phase change material.

4.1. Introduction to Foam-PCM Composites

Real foams are generally a quasi-random network of metal elements which is very difficult to model explicitly. For example, the aluminum foam used in this work is shown in Figure 4.1.

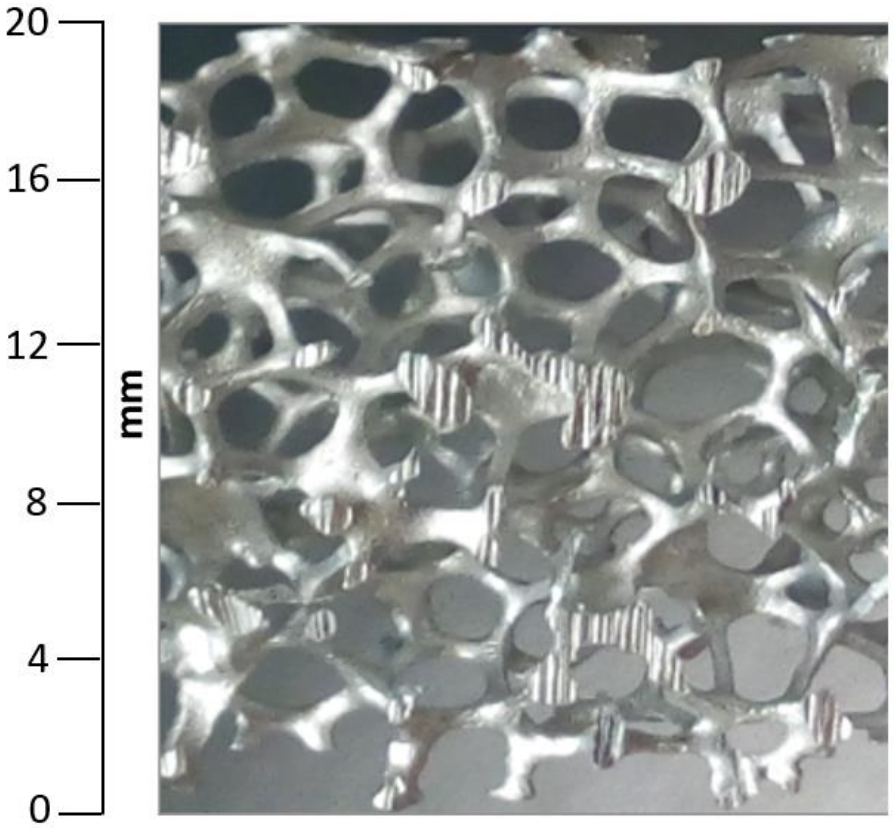

Figure 4.1 Optical photograph of as received aluminum foam

There have been numerous attempts to model foam-PCM composites for predicting thermal performance. Zheng et al. [39] concentrated on pore size simulations of PCM filled in metal foams to compute the overall effective thermal conductivity and simulate the melting process. The copper foam enhanced the effective thermal conductivity of the composite by a factor of 27, and the effective thermal conductivity was found to be higher for lower porosity foams. Trifale et al. [40] modelled foams (similar to ours shown in Figure 4.1) representing a unit cell of the foam as an approximately spherical object made up of 6 square and 8 hexagonal elements. From this geometry, an effective thermal conductivity could be calculated. Mustaffar [21] used a more unconventional technique to obtain the structure of irregular aluminum foam. Specifically, a CT scanner recorded the 3d structure digitally to generate a CAD model (see Figure 4.2) that captures the non-uniform and random nature of the pore structure. Jackson et al. [41] modelled the thermodynamics of foam-PCM composite using a pore-scale sub-model embedded in the larger heat transfer model. They showed that a model can be built without the assumption of local thermal equilibrium between the foam and PCM, making it more accurate and reliable.

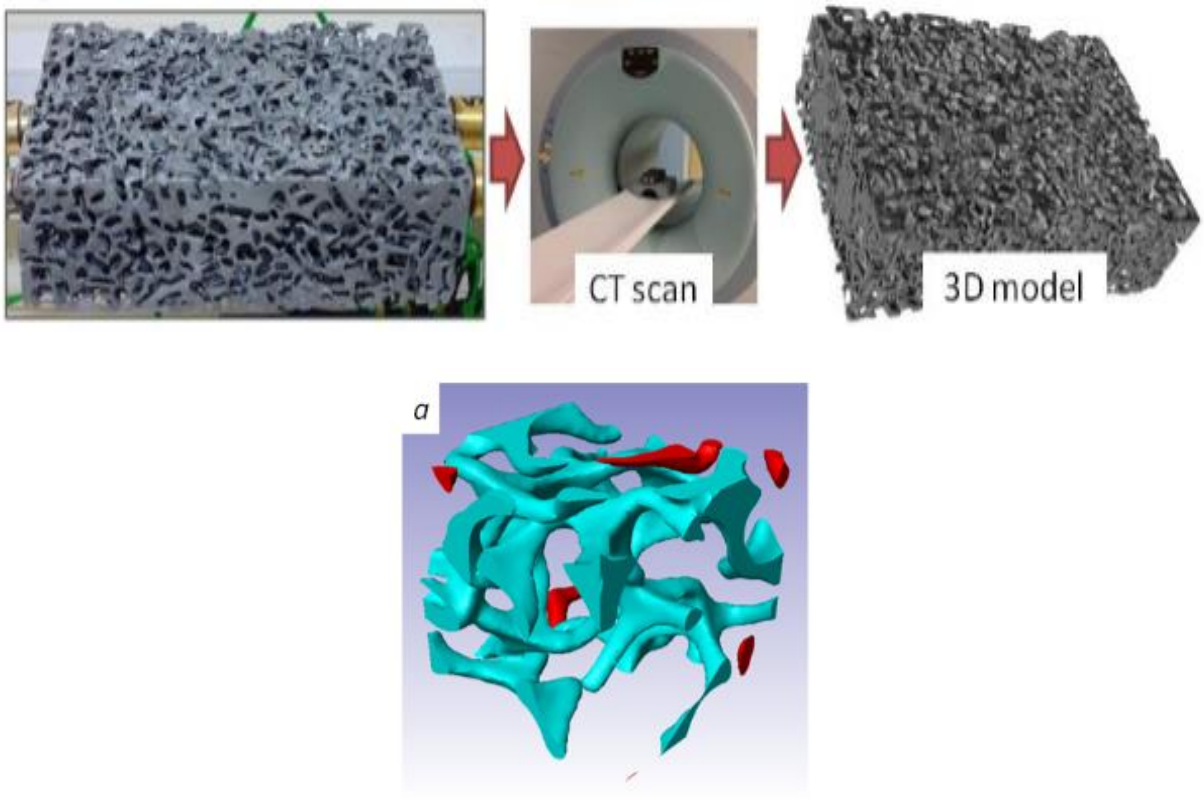

Figure 4.2 Generation of a 3D model using a CT Scan of a foam sample. Figure reproduced from Ref. [21]

But in all of these systems, the thermal resistance between the foam and the phase change material is not accounted for and could significantly impact any predicted thermal conductivity values. Thus, this chapter focuses on experimentally interrogating foam-PCM composites with the goal of understanding the solid-PCM interaction and any potential impact of the interface resistances.

4.2. Applications in Thermal Energy Storage

Heat spreading using foams has been demonstrated to be advantageous for thermal storage applications. Researchers have also studied the combination of graphite foams and phase change materials for thermal energy storage. For example, Kim et al [42] designed a system, which employs channels to carry heat transfer fluid, which are immersed in a matrix of Phase change material and graphite. The graphite helps in spreading heat, which improves the phase change response. It was concluded that, with the addition of the matrix, the number of pipes required was reduced by 92.6%

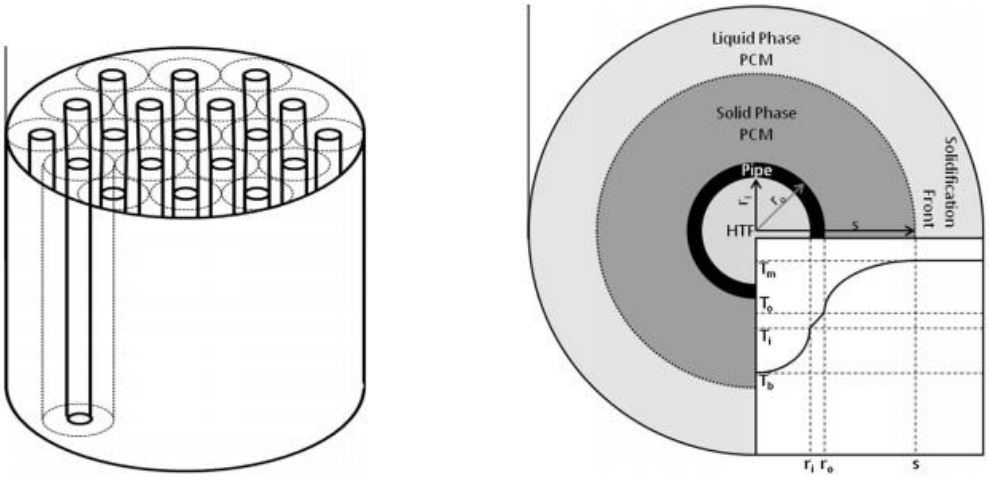

Figure 4.3 Left: LHTES System (The pipes are embedded in the PCM/Foam composite). Right: Solidification of the PCM around a pipe [43]

Huang et al. [43] introduced nickel and copper foams to improve the effective thermal conductivity of PCMs for solar thermal energy storage application increasing the thermal conductivity by a factor of 1.80 and 7.51, respectively. Smaller pores had higher thermal conductivity for both the nickel and copper foam composites Singh et al. [44] used modules consisting of pipes embedded

within graphite foam-NaCl PCMs for concentrated solar power. With the graphite foams, the number of heat transfer pipes inside the modules was reduced by a factor of 12, reducing cost and making the system more compact. To summarize, past work clearly showed the promise of foams for highly responsive thermal energy storage systems highlighting that the foam structure could impact performance.

4.3. Design of a Testbed for Foam-PCM Composites

This portion of the thesis focuses on testing metal foam-PCM composites during charging and discharging with conventional thermal measurements and high resolution thermal imaging to observe the interaction between the PCM and the solid metal foams.

4.3.1 Objectives

In particular, this work aims to understand the transient thermal behavior of a metal foam-PCM composite system heated and cooled with a heat transfer fluid in a concentric cylindrical cell arrangement. Key targets for investigation include the spatially varying temperature response of the composite PCM, compared to pure PCM, the local temperature gradients across the metal-PCM interfaces, and the effect of pore size on the transient parameters.

4.3.2 Key Design & Experimental Considerations

The proposed energy storage system consists of two concentric cylindrical pipes. The inner cylindrical pipe is filled with PCM and a heat transfer fluid flows in the gap between the inner and outer pipes to charge and discharge the PCM. Here, to enable measurements with the infrared microscope, the geometry is split in half along the axis of the cylinder enabling direct optical access to the PCM chamber as shown in Figure 4.4. Thus, the test geometry consists of a half cylinder of PCM with half the annular portion for flow of the heat transfer fluid. The inner tube is shorter than the outer one to form an inlet and outlet housing for the fluid. The center portion of the test fixture is isolated from the endcaps with half cylinders made of aluminum such that in the test section the flow in the annulus has approximately 1D, fully developed flow conditions. An external insulation made of acrylic is added to minimize the convection losses.

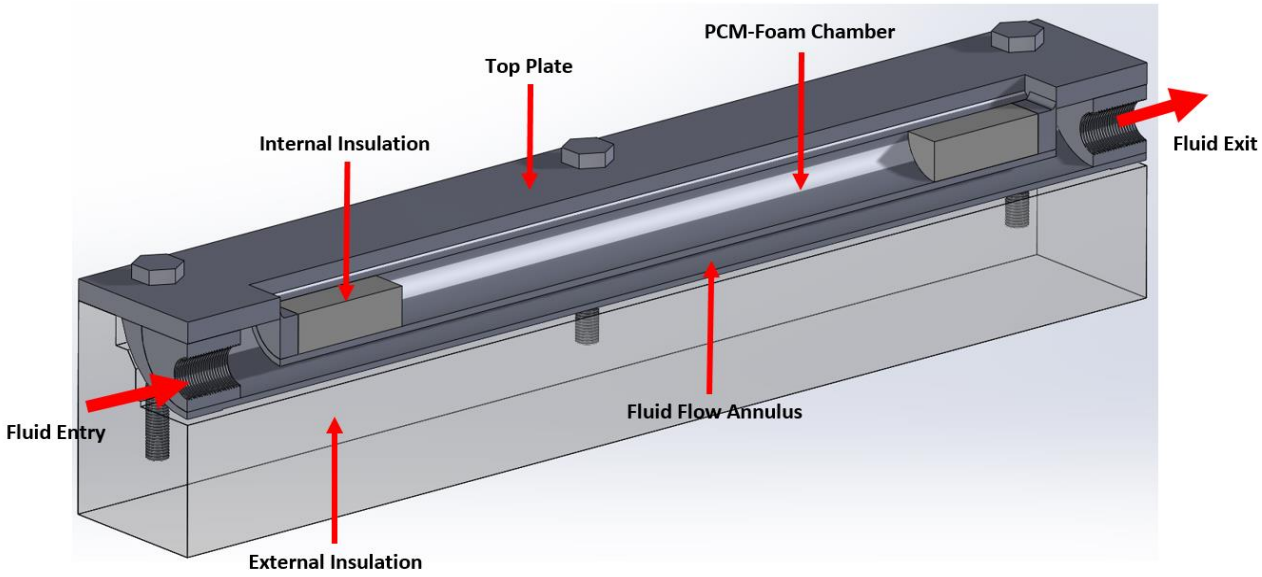

Figure 4.4 Cross-sectioned schematic of the test fixture. The PCM is contained within a half-cylinder chamber at the top of the text fixture. A heat transfer fluid enters the annular flow section and travels along the length of the chamber. Internal insulation is placed at either end of the PCM chamber to ensure that flow in the annular region is approximately 1D and fully. developed in the observed test section

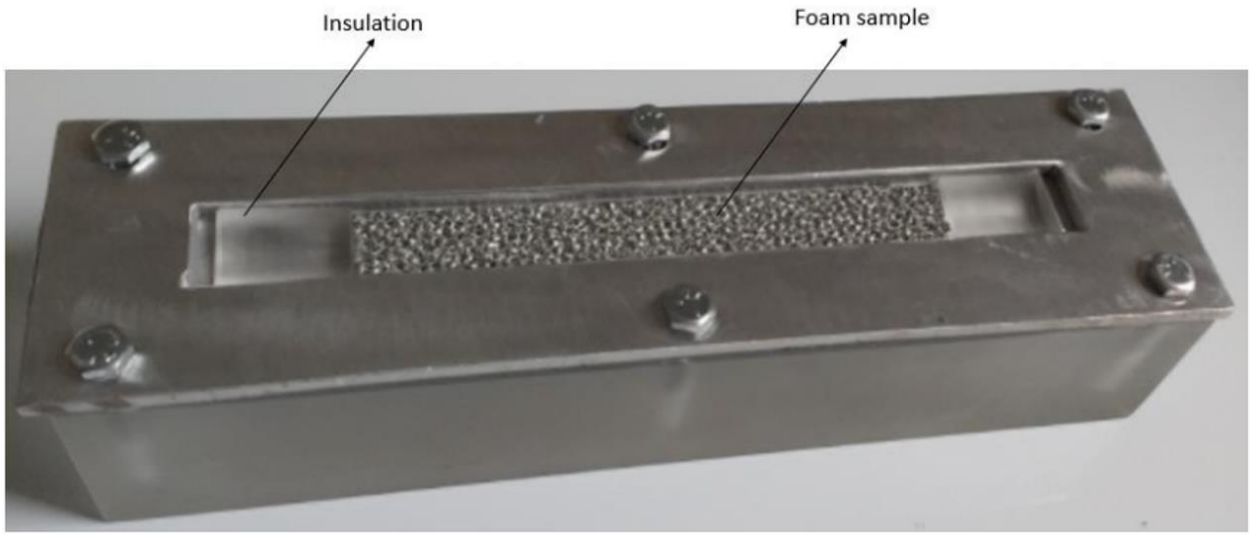

Figure 4.5 As built test rig containing one of the foam samples. The transparent acrylic insulation can be seen on either end, which block heat transfer from the sides to approximate a 1D Heat flow. Good contact between the foam sample and the chamber is ensured to avoid a significant contact resistance, which can disrupt heat flow

A heat transfer fluid consists of a mixture 90% Ethylene Glycol (EG) and 10% water (see Appendix for properties) and was chosen for several reasons:

1) The boiling point is above the required set point in the chiller during melting cycle.
2) Its freezing point is below the required set point in the chiller during solidification cycle.
3) Its viscosity range is within the range that can be handled by the experiment equipment including the flow meter and pump system.
4) It has reasonable heat transfer properties including thermal conductivity and specific heat.
5) It is commercially available for a reasonable price.
6) It is compatible with the materials used in the test rig and the piping.
7) It can be easily cleaned.

The experiments consist of both a charging and discharging cycle with thermocouple measurements of fluid and rig temperatures, flow rate measurements, and thermal imaging with the infrared microscope. Initially, the entire system is charged to 100^{o}C while observing the melting behavior. Then, the system is discharged using a cooling fluid with an inlet temperature of ~10^{o}C. Because the EG-Water solution has a temperature dependent viscosity, the maximum flow rate is ~2.2 GPM for charging (melting) cycle and 0.5 GPM during discharging (solidification). For design calculations, we estimate a natural convective heat transfer coefficient of 5 W/m^2-K from all exposed surfaces. The phase change temperature for the selected PCM (PureTemp 42) is ~42^{o}C with an approximately a 3K transition range.

4.3.4 Metal Foams

Half-cylinders of metal foams were procured from ERG Aerospace Company (see Figure 4.6) Two sets each of 5, 10, 20, and 40 PPI were ordered. The foams have a relative density of 7-9 %. The material is Aluminum heated to T6 condition (anodized). The foams were polished at the end to make sure a tight fit is ensured at the ends and at the curved surface which is in contact with the cavity.

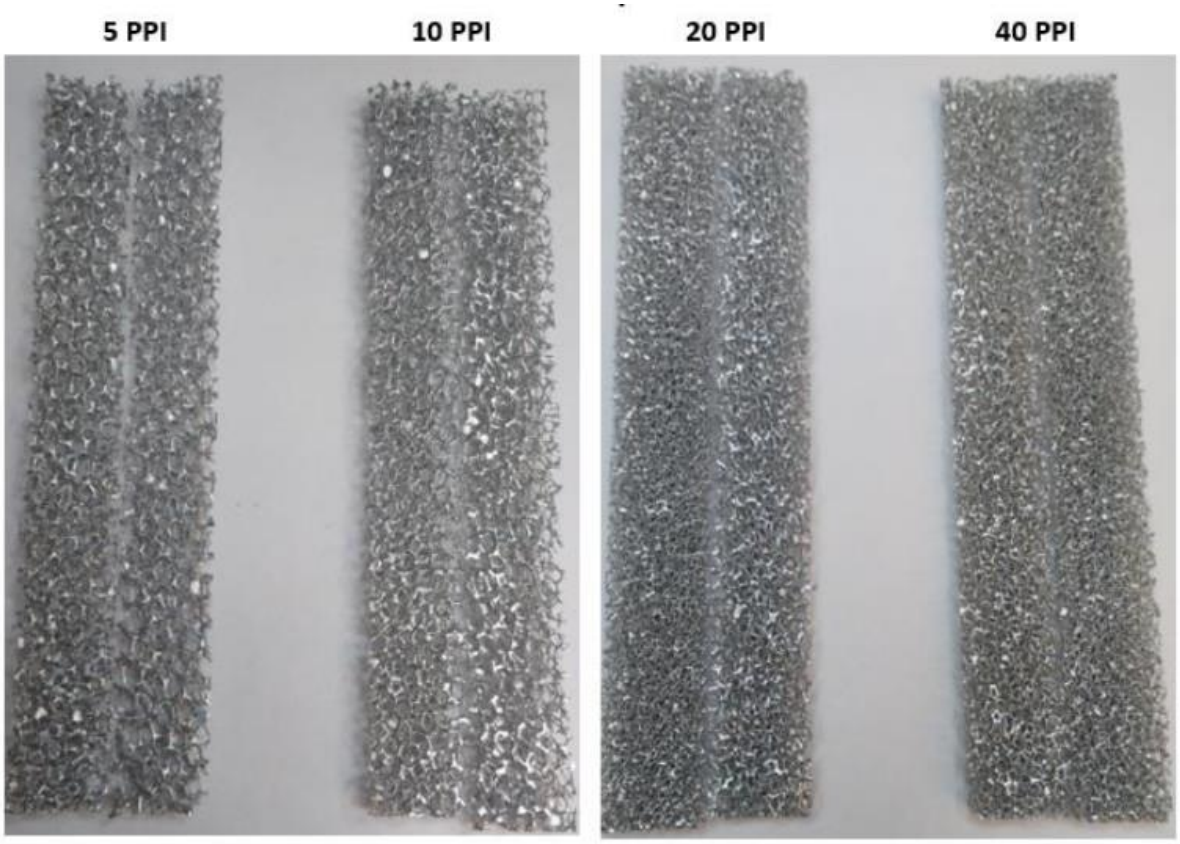

Figure 4.6 Optical photograph of the as received foam samples from ERG Aerospace. Each half cylinder has a diameter of 20 mm and a length of 150 mm

4.3.5 CFD Simulations

To optimize the flow channel design, CFD Simulations were carried out using ANSYS. Specifically, the simulations enabled us to evaluate the entry region into the annular flow channel and to observe if it reaches fully developed flow in region of interest of the test section.

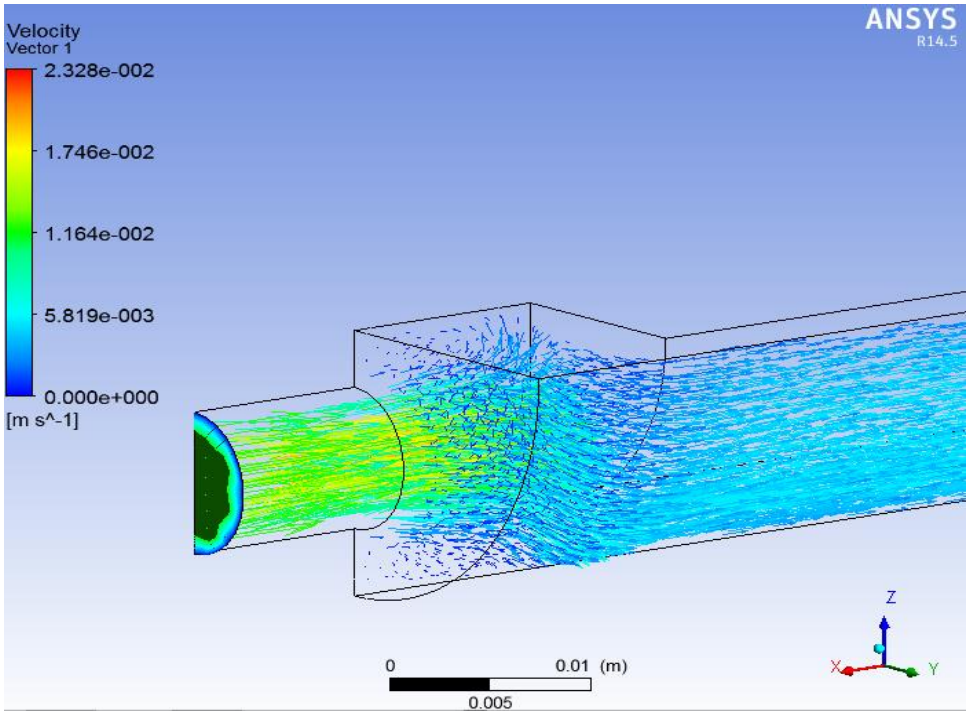

Figure 4.7 Flow visualization (velocity vectors) at the entry to the annular flow cavity

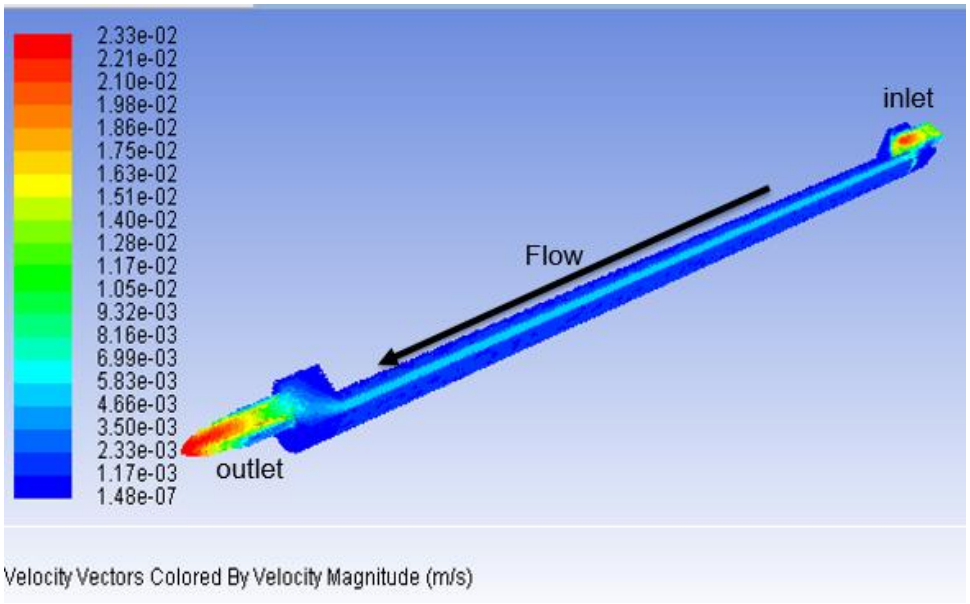

Figure 4.8 Flow simulation at steady state across the entire length of the flow section with color indicating flow velocity. This simulation was used to size the length of the insulation regions at the inlet and outlet to ensure the test section had approximately fully developed flow in the annulus

4.4. Experimental Procedure

4.4.1 Flow Loop:

The experimental target for to mimic the thermal storage application is to prime to 100^{o}C during charging (melting), then cool with a fluid at 10^{o}C to discharge the sample (solidification). Quick swapping between the two temperature ranges is required. Thus, two fluid reservoirs and a system of values as shown in Figure 4.9 was designed and ensures the quick swapping of the working fluid in the main line. The values are manually opened and closed such that the working fluid is switched from the hot reservoir to the cold reservoir within a few seconds. Due to thermal losses in the piping, the hot chiller reservoir is set at 105^{o}C for a fluid inlet temperature at the rig of 90-95^{o}C. Similarly, the cold chiller is set at -10^{o}C, as the fluid temperatures will eventually rise to 10^{o}C after passing through the stains of the left over hot fluid during melting cycle.

Figure 4.9 Left: Temperature controlled reservoirs. The fluid temperature and pump power can be adjusted in each individual reservoir. Right: The value system to ensure quick swapping of fluid

Figure 4.10 illustrates the fluid flow circuit and experimental setup including two fluid reservoirs (to maintain the fluid at fixed hot and cold temperatures for charging and discharging) with pumps to circulate the fluid (max pressure: 4.2 PSI), the network of pipes and values to direct the fluid, a flow meter to measure flow rates, thermocouples probes to measure fluid inlet and outlet temperature, the test rig. The infrared microscope observes the temperatures at the surface of the test fixture during melting and solidification, and a DAQ system logs data from the thermocouples.

High temperature/chemical resistant Buna S Rubber pipes were chosen for the piping. The chiller system can supply a flow rate for 0.5 GPM for solidification and 2.2 GPM for melting for a fixed maximum pump pressure of 4.2 PSI. This is due to changes in fluid viscosity as a result of temperature change.

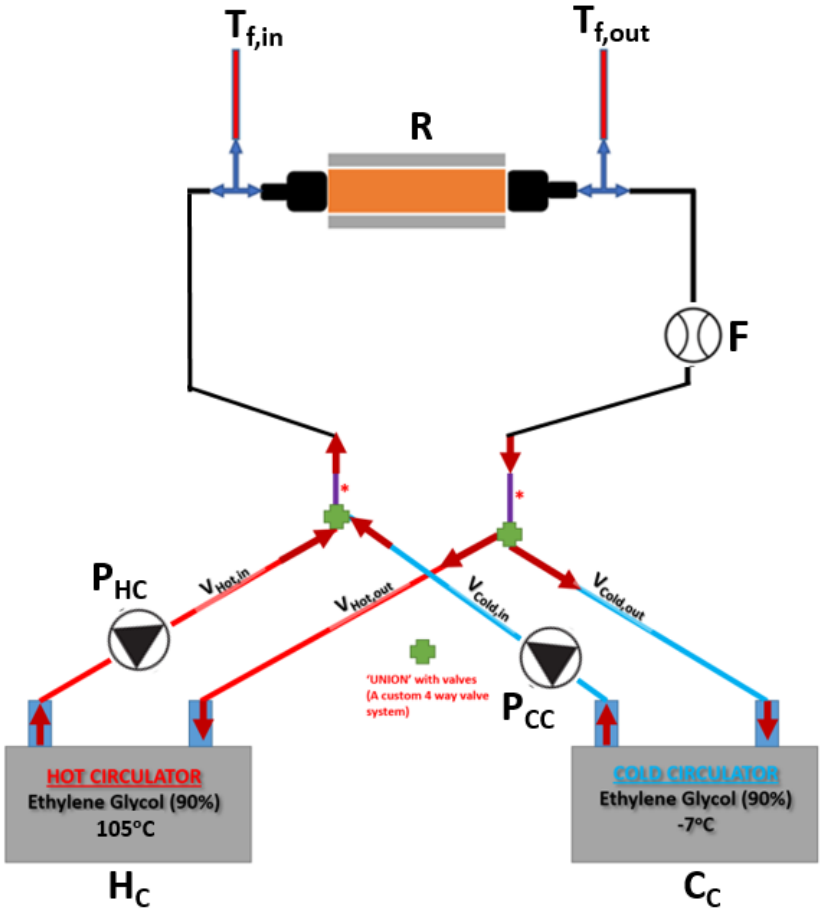

Figure 4.10 Flow circuit consisting of the temperature controlled fluid reservoirs (one for hot fluid (**H_C**), other for cold fluid (**C_C**), the pumps (**P_{HC}** and **P_{CC}**, Rated at 4.2 PSI), (**F**) the flow meter, (**$T_{f,\,in}$, $T_{f,\,out}$**) thermocouples to measure the inlet and outlet fluid temperatures, respectively, and **(R**) the test rig

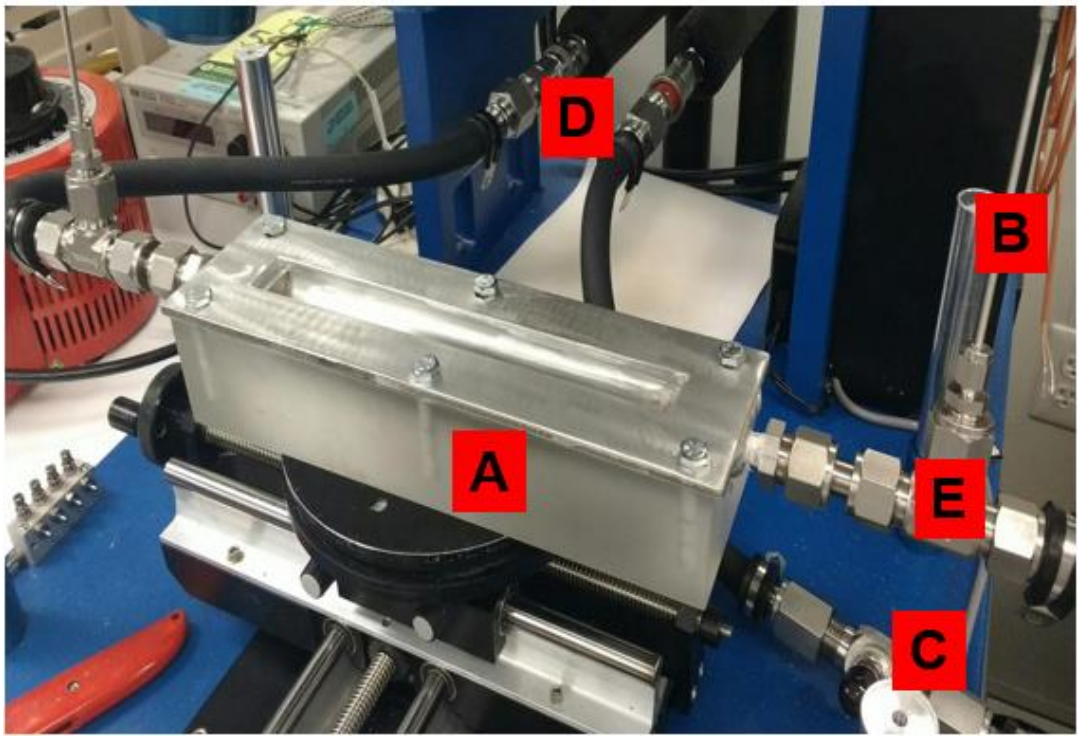

Figure 4.11 Experimental configuration including the (**A**) test rig, **(B)** thermocouples to measure fluid inlet and outlet temperature, (**C**) the flow meter, (**D**) inlet/outlet quick disconnect, and (**E**) the T-joint to house the thermocouple

4.4.2 Infrared thermal imaging

Infrared thermal microscopy is a powerful tool enabling observation of the spatially- and temporally-varying temperature profile on a surface. Here, we use a QFI Infrascope system, which has 5 available magnifications: 1/6x, 1x, 4x, 12x, and 20x enabling a range of spatial resolutions and fields of view. The 1/6x lens observes approximately 40% of the length of the sample in a single image with 105 μm spatial resolution.

Figure 4.12 The QFI Infrascope IR Microscope

4.5. Experimental Analysis of Phase Change in foams

Here, four samples are analyzed to understand the impact of foams on the phase change process and to evaluate the impact of pore size (5, 10, and 200 PPI) on the performance of the system. For each sample, the melting and solidification behavior is observed and analyzed, and for the foam composite samples, we focus on the interaction of the PCM and foam.

4.5.1 PCM Only:

As a benchmark, we first evaluate the case without the foam. Three monitoring points spaced evenly across the breadth of the channel are chosen for further analysis and comparison (see Figure 4.13(a)): (a) at the 6.67 mm from the top edge of the channel, (b) at the center of the channel (10 mm), and (c) at 13.2 mm from the top edge of the channel. The phase change duration depends on the location along the breadth of the sample (see Figure 4.13(b)). The points near the edge solidify faster than the centerline. Heat must diffuse from the center to the edge during solidification and the thermal resistance to dissipation increases with distance from the cold walls. This is further

highlighted in the thermal maps shown in Figure 4.14. Note that the solidification is not 1-D radially, but the solidification front also moves from the inlet to the outlet.

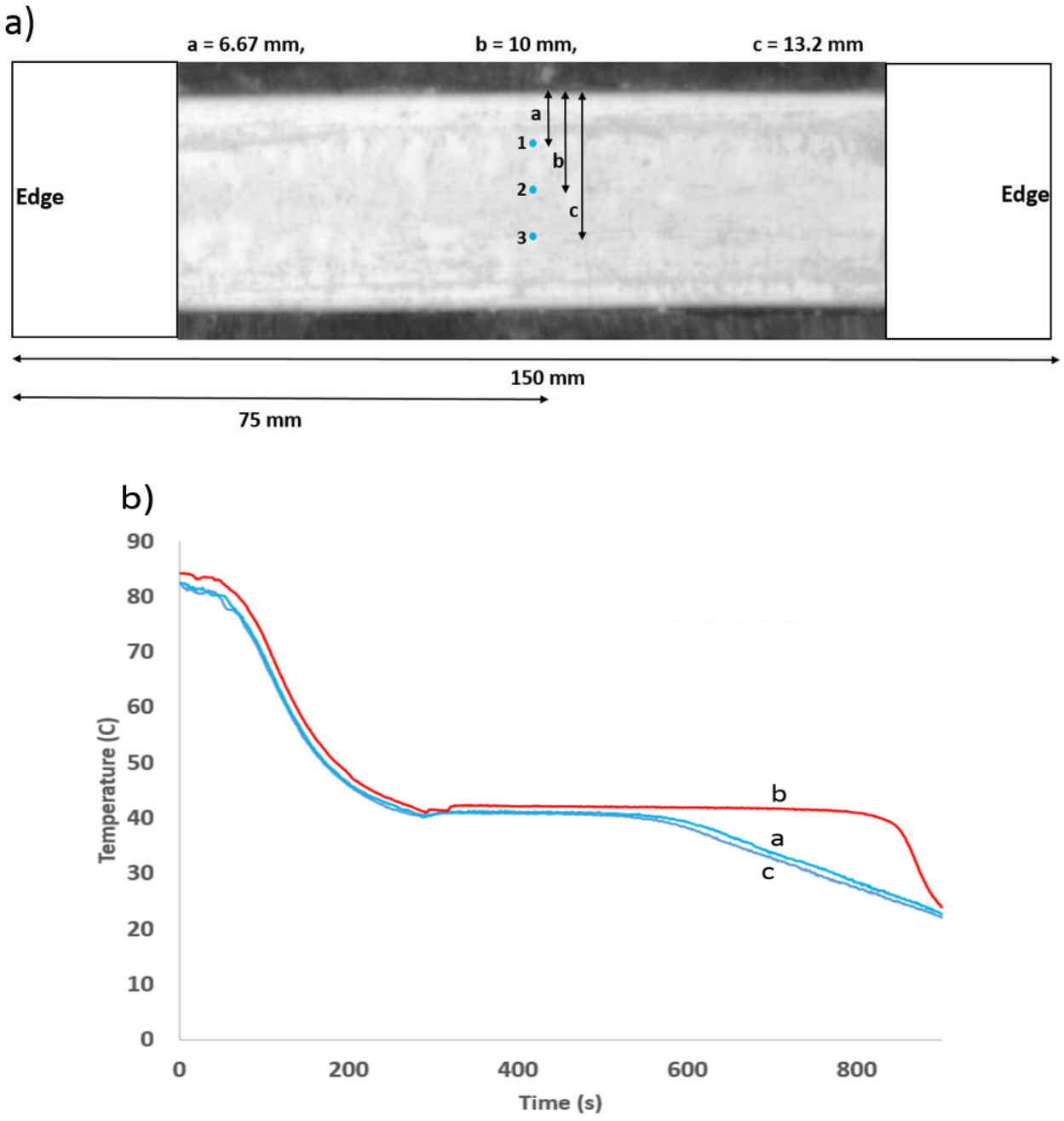

Figure 4.13 (a) Infrared radiance image with selected monitoring points identified and (b) corresponding temperature history during the solidification process. Within the radiance image, the bright region corresponds to the phase change material; the dark regions are the aluminum plate. The microscope observes a region approximately 75 mm long near the center of the test fixture. Monitoring points (a) and (c) have similar temperature histories demonstrating the symmetry of the process about the centerline

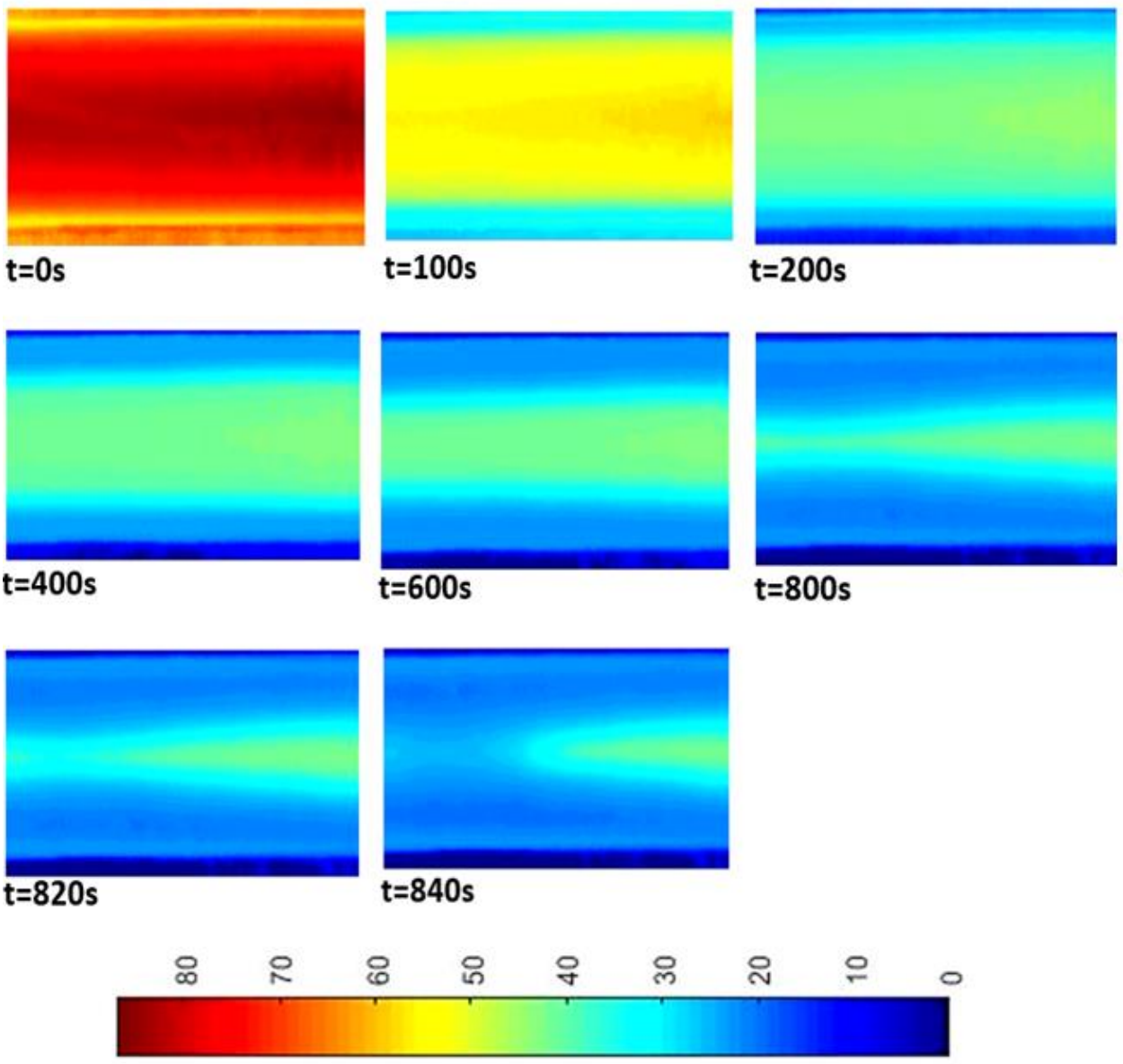

Figure 4.14 IR thermal maps during the solidification cycle for the PCM only case. Note that the solidification front moves both inward from the aluminum walls (towards the center) and lengthwise from the inlet (left) to the outlet (right).

4.5.2 5PPI Foam:

The 5 ppi foam has a network of pores which are separated by an average of 5mm. The phase change material is infiltrated into the pores in the molten state and allowed to solidify. The focus radiance thermal image taken is shown in Figure 4.15 along with 3 selected monitoring points in the foam and 3 in the PCM regions. We observe the foam as metal islands (dark spots) protruding from the PCM. The PCM is charged up to the surface in stages. The monitoring points are selected in such a way that they are approximately uniformly spaced across the breadth of the sample. Three points in PCM region and three points in the foam region are selected.

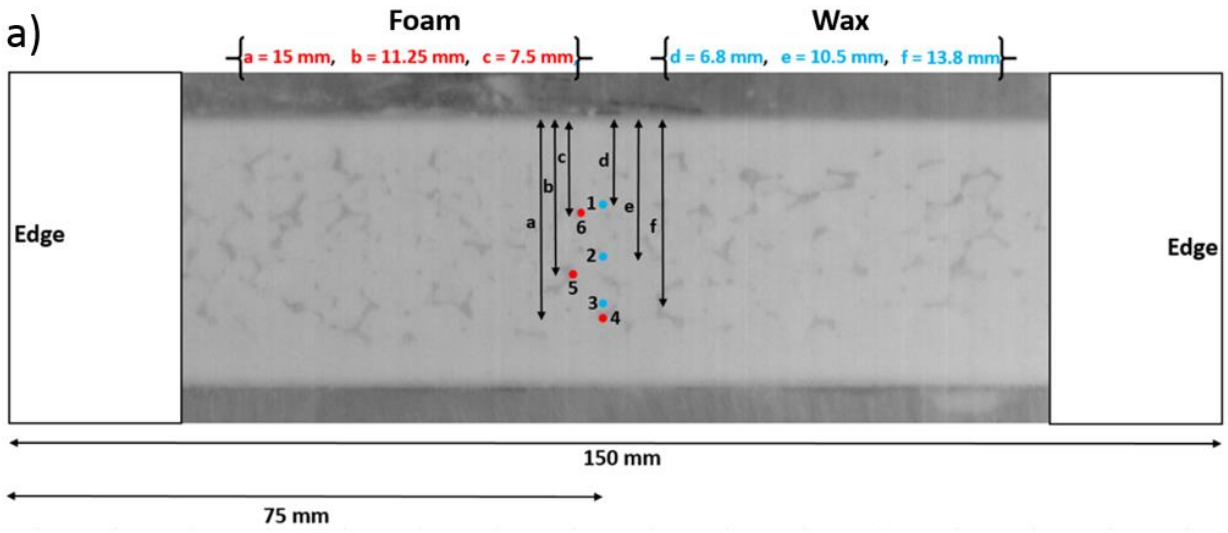

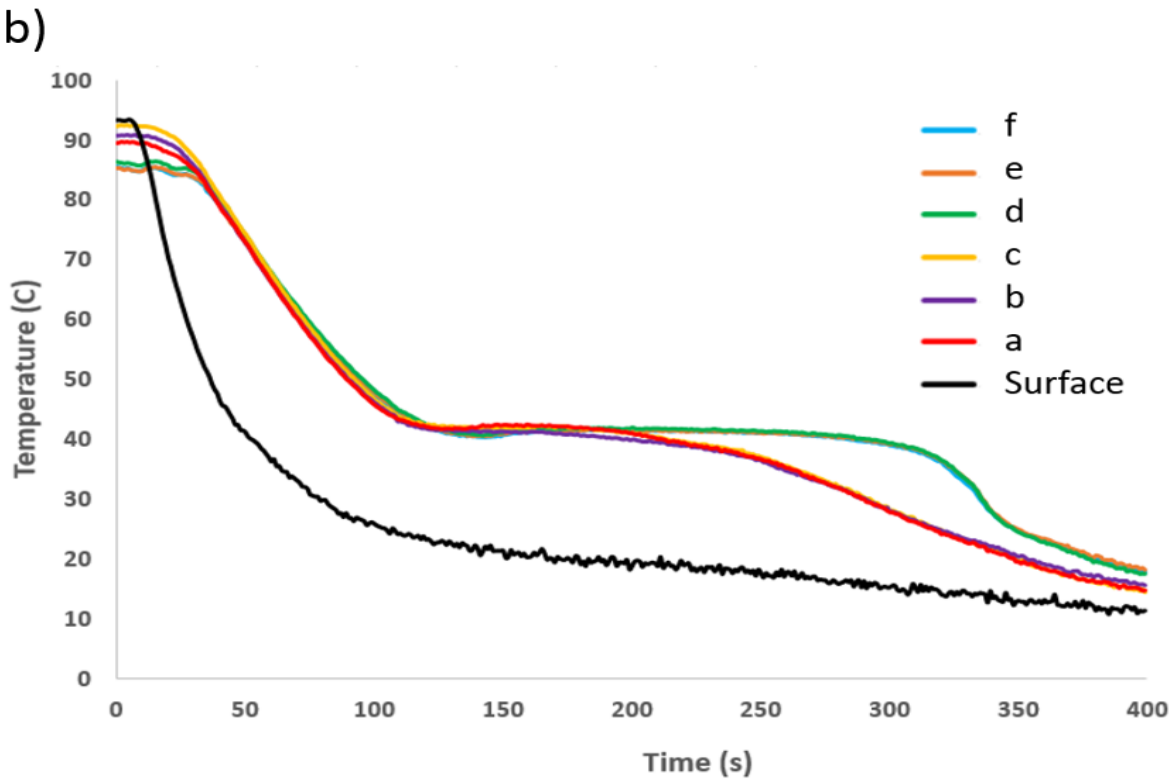

Figure 4.15 (a) Infrared radiance image for the 5PPI foam composite with selected monitoring points identified and (b) corresponding temperature history during the solidification process. In the radiance image, dark spots within the bright PCM region are the ends and edges of the metal foam. From temperature history in (b), it is clear that the temperature is fairly uniform throughout the PCM with the introduction of the foam

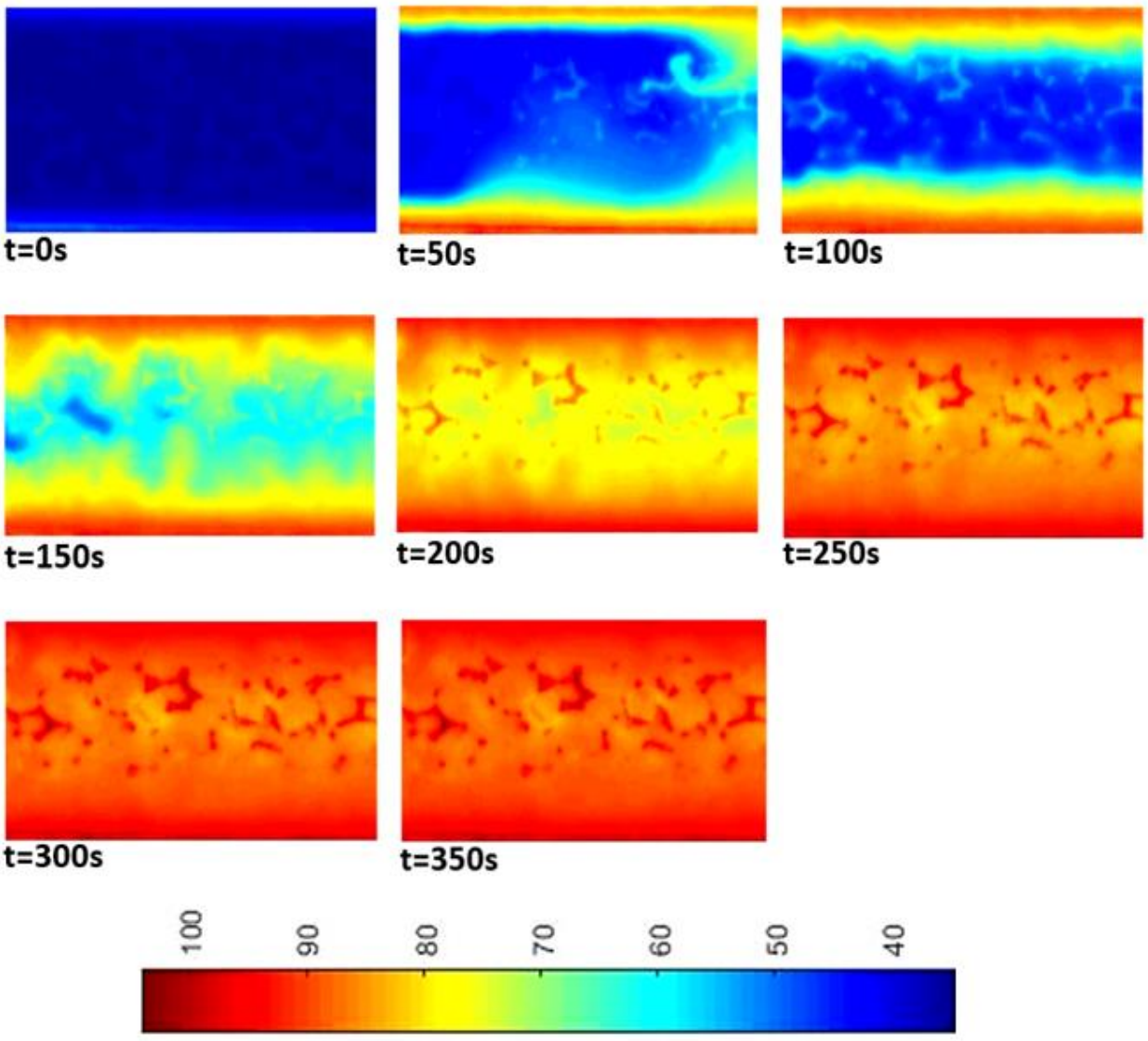

Figure 4.16 IR thermal images taken during melting cycle for 5 PPI Foam sample. Note that the melting occurs in the foam pores thereby speeding up the process. The melt fronts start from the sides and progress inwards (towards the center)

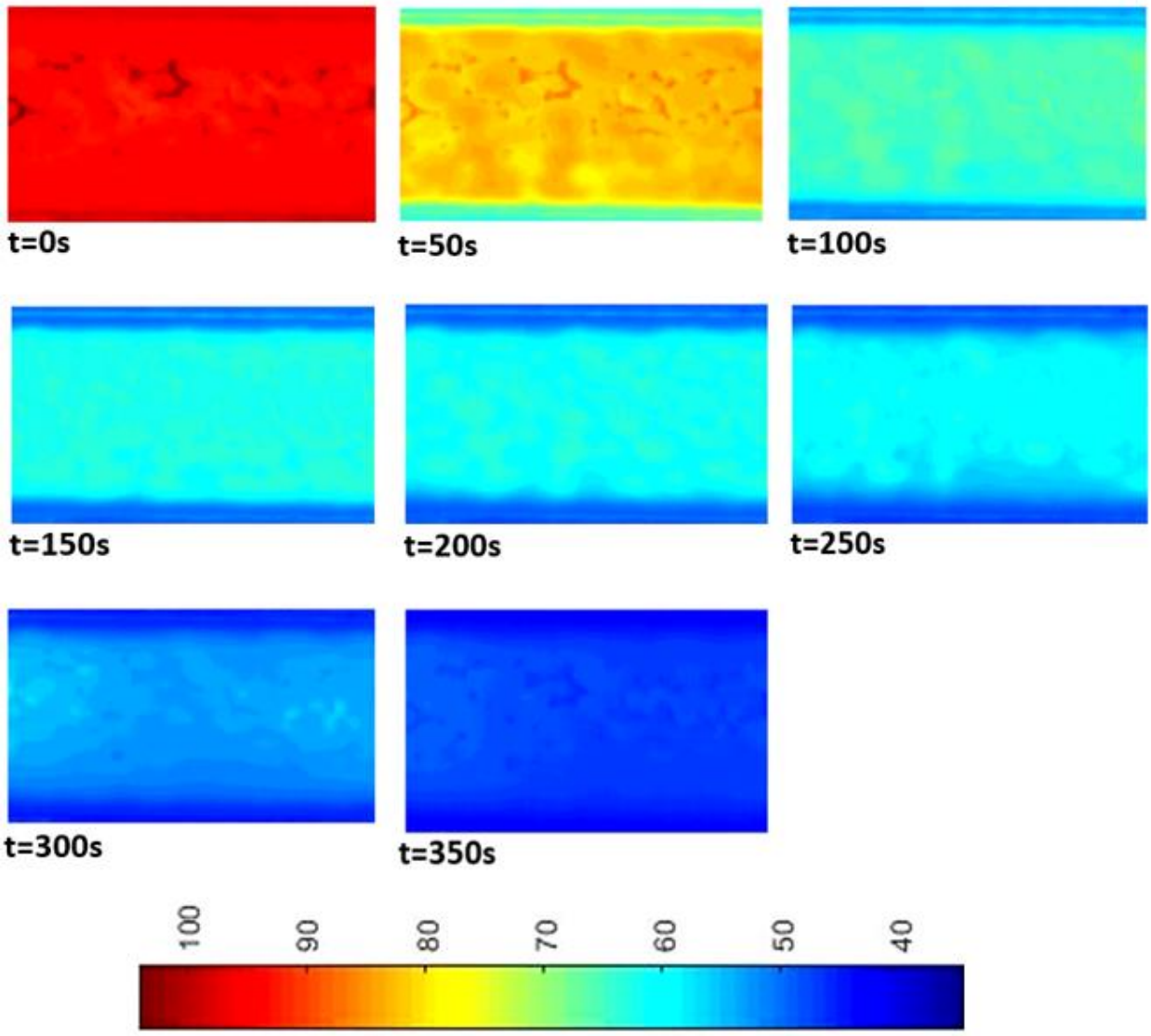

Figure 4.17 IR Images taken during solidification cycle for 5 PPI Foam sample. Note that solidification is localized in small concentrated spots, which are between the foam elements, there by speeding up the process. Once again, the solidification front begins from the sides and progress towards the center

4.5.3 10 PPI Foam:

The 10 PPI foams have pore sizes 2.5 mm. The infiltration of phase change material is similar to that of the 5 PPI sample. The focus radiance thermal image taken is shown in Figure 4.18 along with 3 selected monitoring points in the foam and 3 in the PCM regions. The PCM is charged up to the surface in stages. The monitoring points are selected in such a way that they are uniformly spaced across the breadth of the sample. Once again, three points in PCM region and three points in the foam region are selected. We can observe that the solidification time for the 10ppi foam sample is slightly lower compared to the 5ppi sample. Here the time is around 300s.

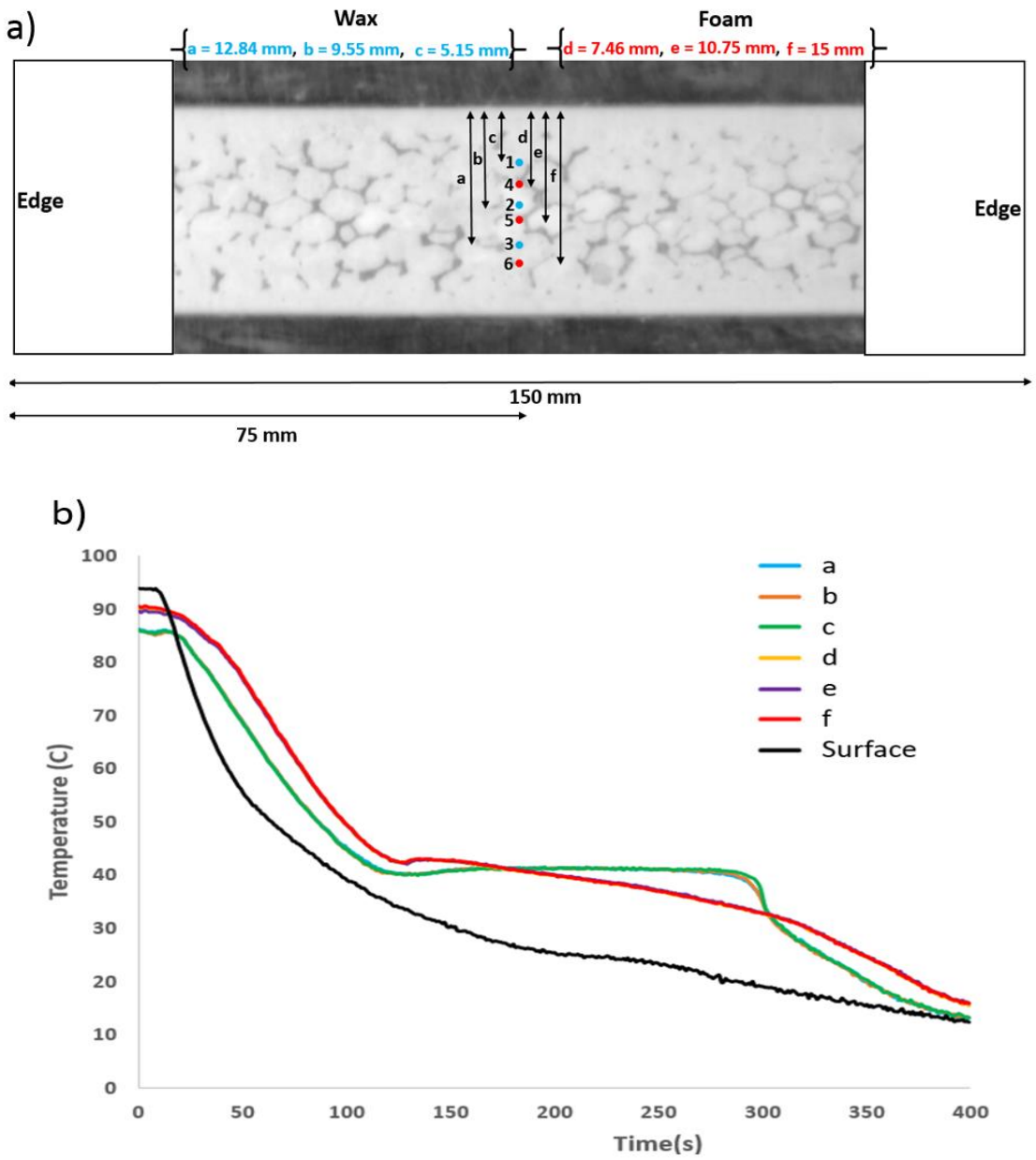

Figure 4.18 (a) Infrared radiance image for the 10PPI foam composite with selected monitoring points identified and (b) corresponding temperature history during the solidification process. In the radiance image, dark spots within the bright PCM region are the ends and edges of the metal foam. From temperature history in (b), it is clear that the temperature is fairly uniform throughout the PCM with the introduction of the foam just as in 5PPI sample

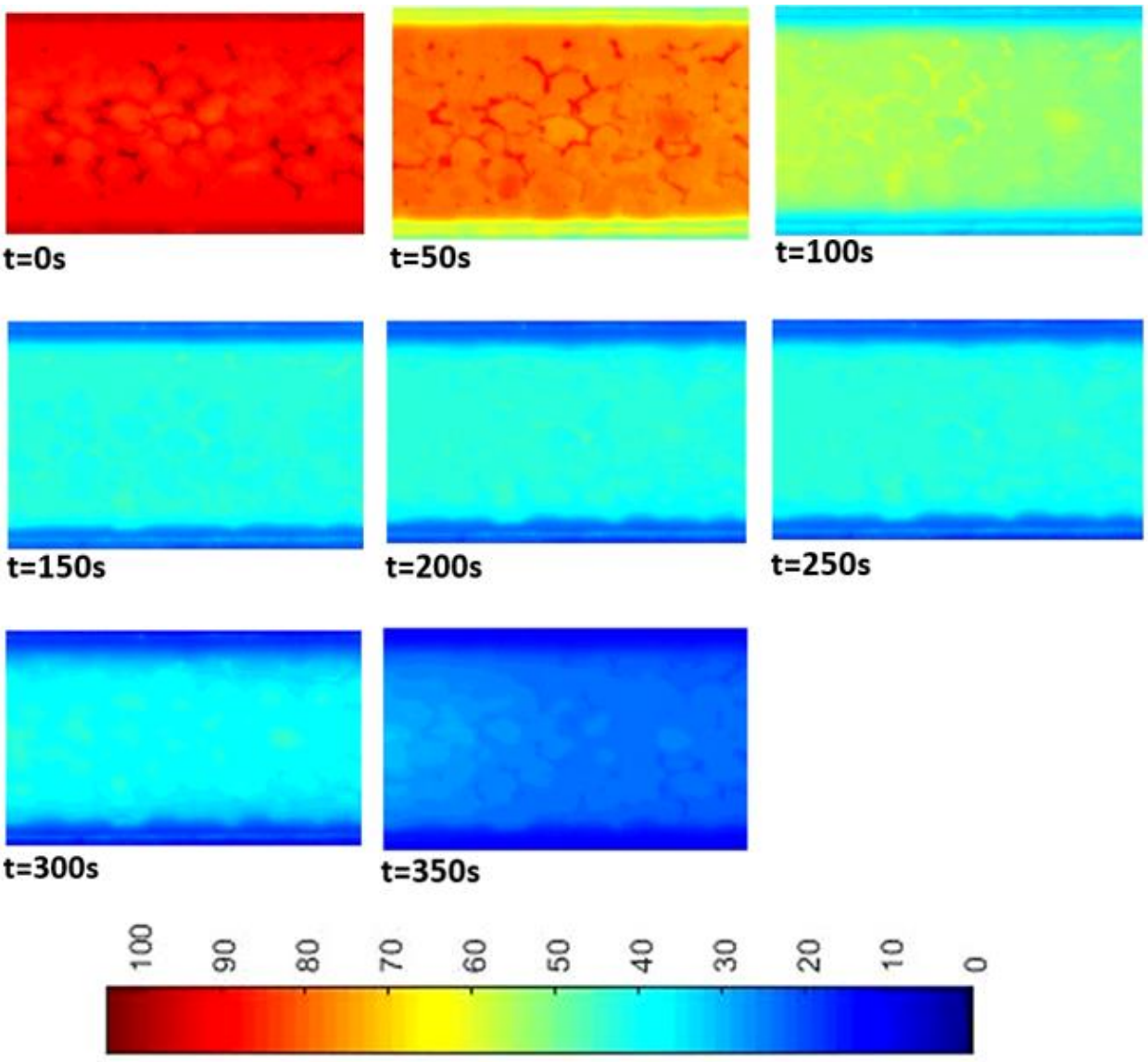

Figure 4.19 IR Images taken during solidification cycle for 10 PPI Foam sample. We can again see the solidification happening in the foam pores. In this case, since the pores density is higher, the solidification occurs faster compared to the 5PPI Foam sample

4.5.4 20 PPI Foam:

The 20 PPI foams have pore sizes of about 1.25 mm. The focus radiance thermal image taken is shown in Figure 4.20 along with 3 selected monitoring points in the foam and 3 in the PCM regions. We can see that the spots are densely populated unlike the 5 and 10 PPI foams. The PCM is charged up to the surface in stages. The monitoring points are selected in such a way that they are uniformly spaced across the breadth of the sample. Three points in PCM region and three points

in the foam region are selected. The solidification time for the 20 PPI foam is lower than the 10 and 5 PPI foam. It is about 290s.

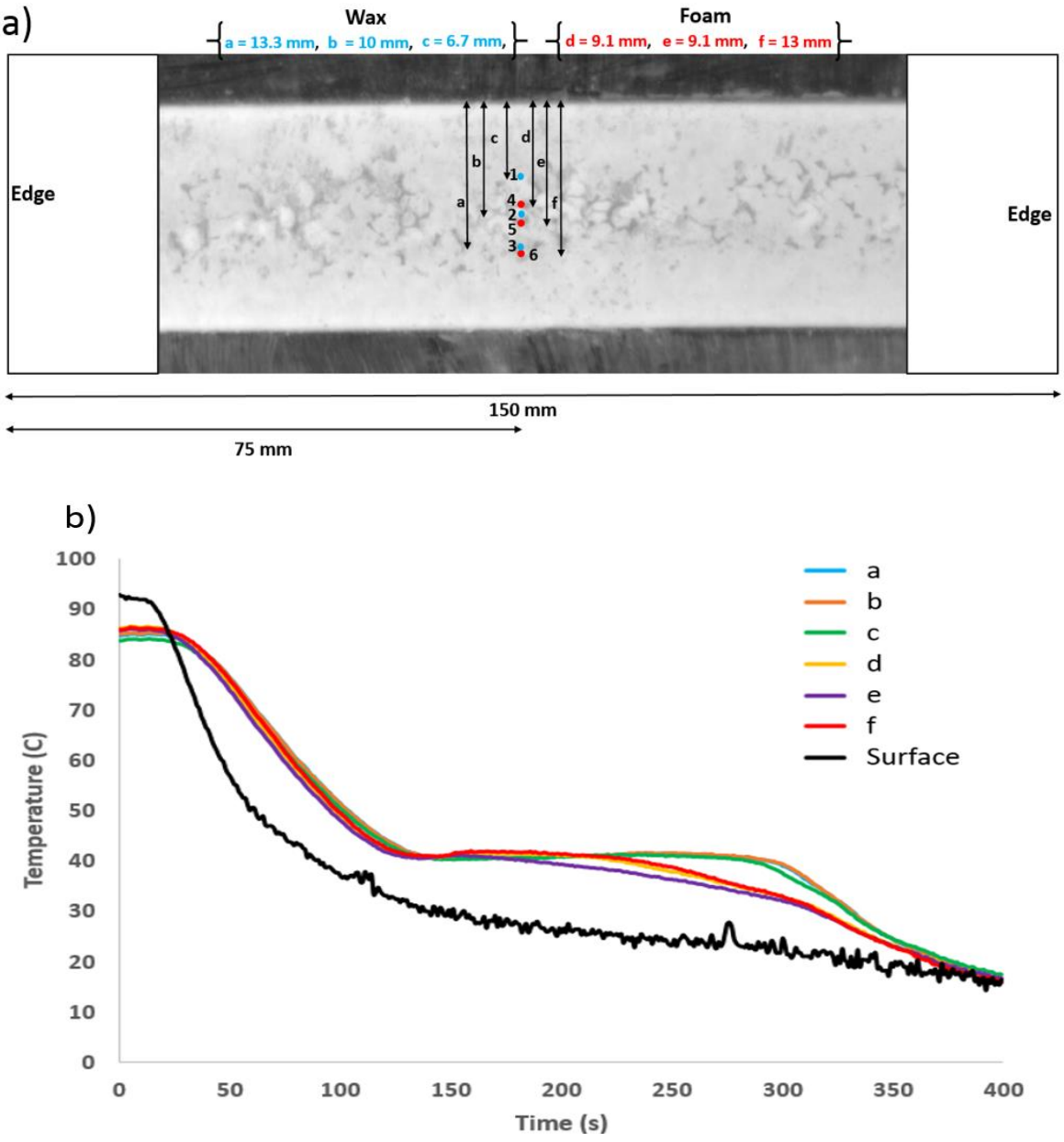

Figure 4.20 (a) Infrared radiance image for the 20PPI foam composite with selected monitoring points identified and (b) corresponding temperature history during the solidification process. In the radiance image, dark spots within the bright PCM region are the ends and edges of the metal foam. From temperature history in (b), it is again clear that the temperature is fairly uniform throughout the PCM with the introduction of the foam just as in 5 and 10 PPI sample

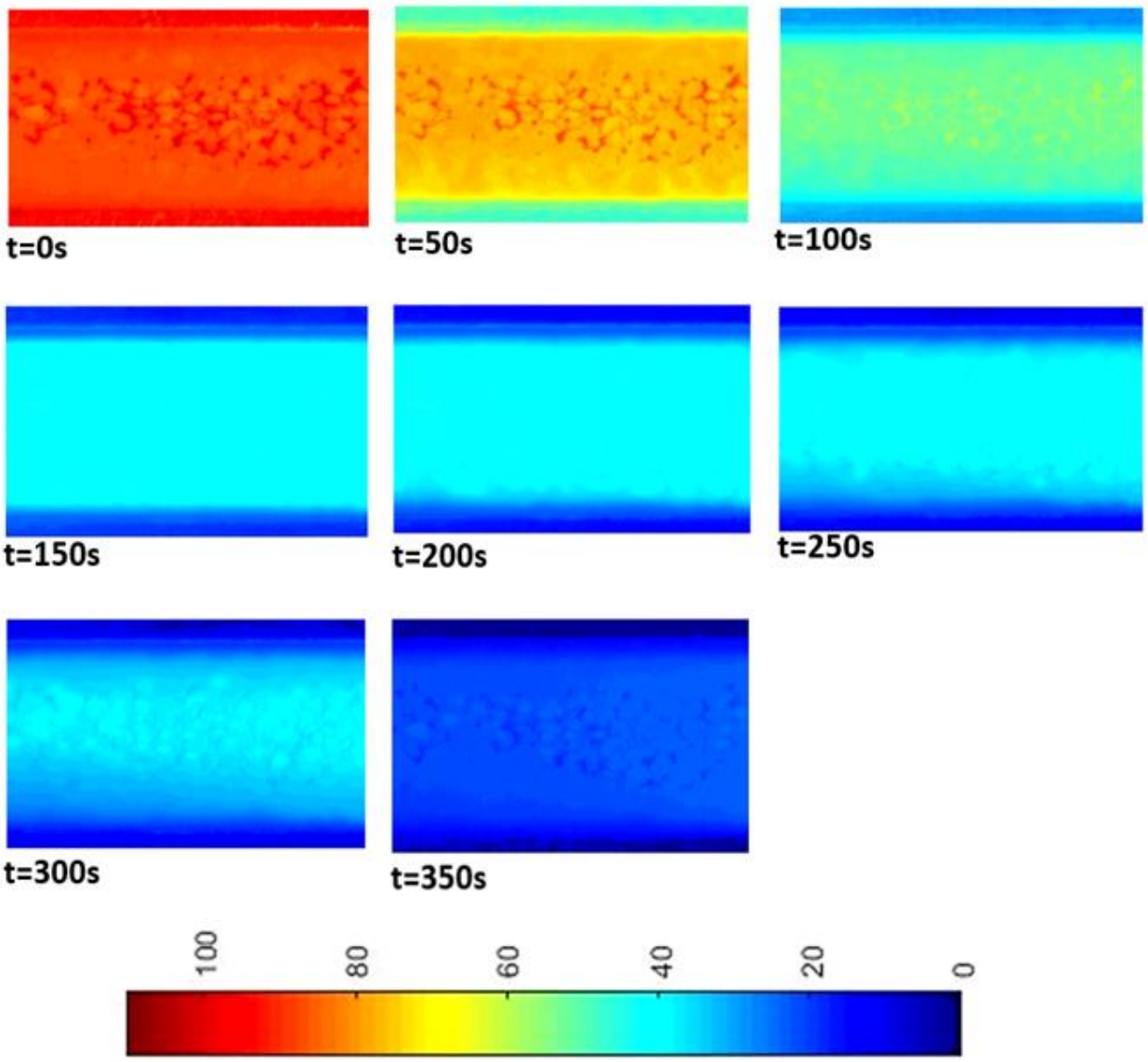

Figure 4.21 IR Images taken during solidification cycle for 10 PPI Foam sample. We can observe the island formation better than 5 or 10 PPI samples, which makes solidification; occur quickest amongst all the samples

4.5.5 Comparison of Solidification Times

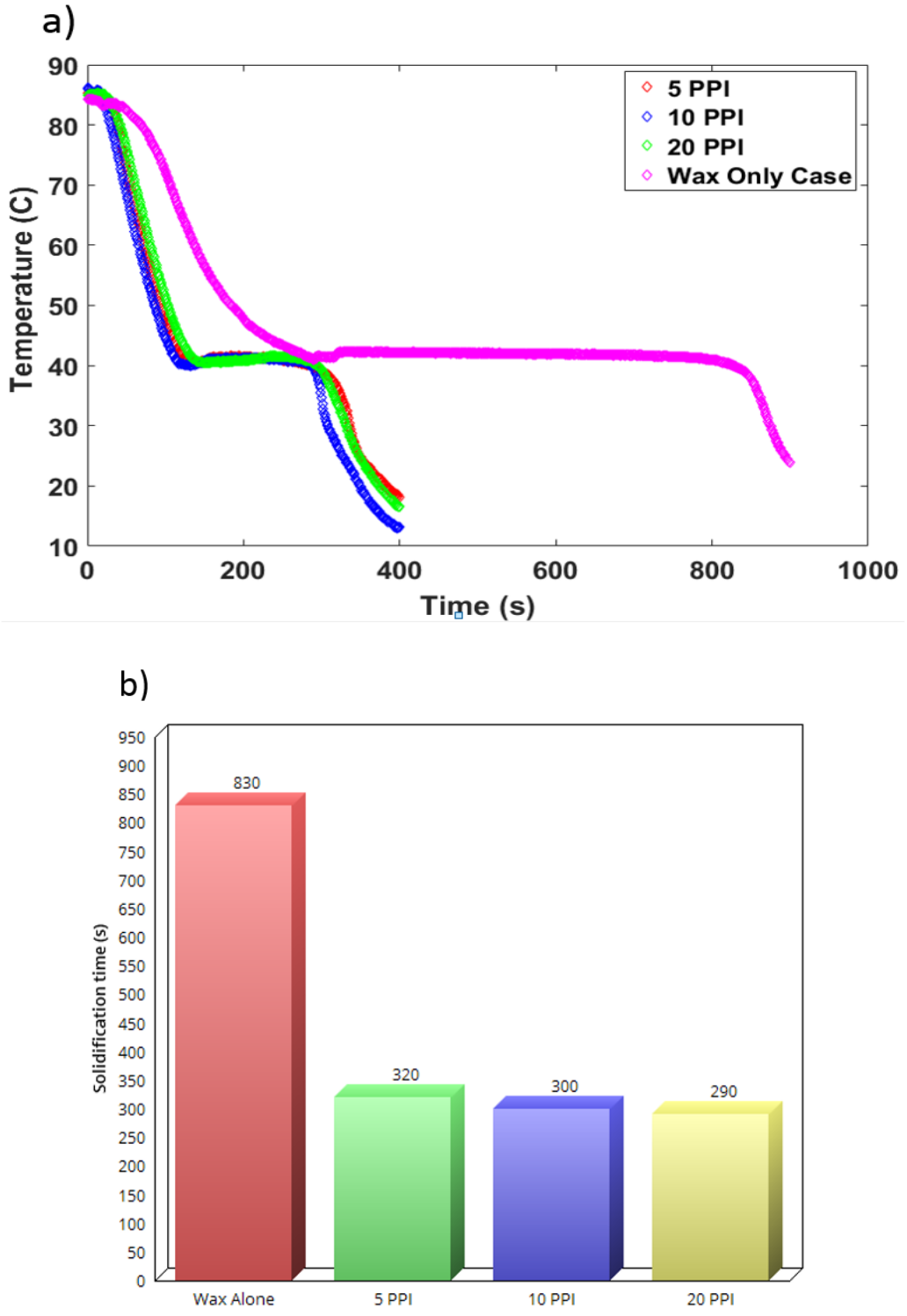

Figure 4.22 (a) Centerline temperature evolution in the PCM during solidification and (b) time for solidification at the center monitoring point

In all cases, the temperature plateaus at the phase change temperature of 42^{o}C until the discharging cycle is completed (see Figure 4.22). With foams, the solidification time is approximately 300s, while for the PCM alone it is 830ss. Foams reduce the phase change response time of the PCM-Foam system by 2.8 times. Within the foam, the PCM is confined to pores and the phase change is now more localized that occurs much quicker as compared to the bulk PCM system. The improved phase change response is attributed to the heat spreading capability of high conductivity foams, which enhances the effective thermal conductivity of the system. Note that the foam temperature curves follow a similar trend as the monitoring points chosen are near to the PCM-Foam interface. But they drop at a faster rate as they are not affected by phase transition.

4.5.6 Rate of Latent Heat Recovery

We calculate the rate at which heat can be recovered from each foam sample from the amount of phase change or the rate of change of the PCM mass from liquid to solid per second. This can be obtained by dividing the amount of energy used for phase change by the solidification time for the specific sample. Since the amount of PCM is roughly the same for all cases, the rate depends on the solidification time.

Wax only case : $\text{Rate of Heat Recovery}_{\text{latent}} = (m_{pcm} L_{pcm})/t_{\text{phase change}}$ (1)

Cases with foams : $\text{Rate of Heat Recovery}_{\text{latent}} = \varepsilon\, m_{pcm}\, L_{pcm}/t_{\text{phase change}}$ (2)

where L_{pcm} is the latent heat of PureTemp 42, m_{pcm} is the amount of PCM used in the PCM only case, $t_{\text{phase change}}$ is the average time of solidification, and ε is the porosity of the foam sample used.

The rate of heat recovery increases with foams and increases slightly as the pore size is decreased. However, only a small range of pore sizes was considered and additional analysis of larger and smaller pores is required to make conclusions about the impact of pore size.

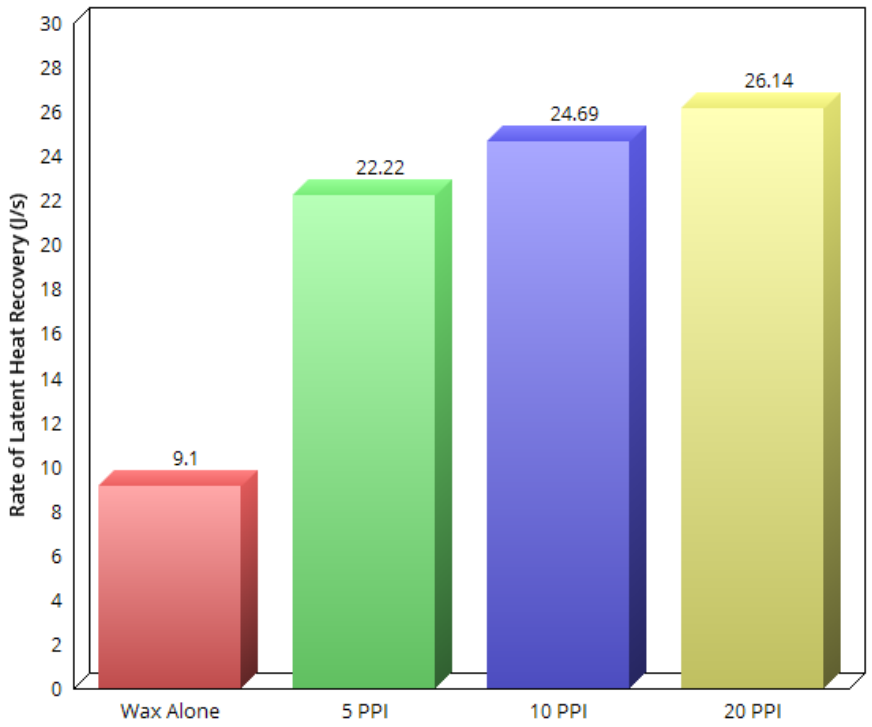

Figure 4.23 Impact of foam pore size the approximate rate of heat recovery

4.5.7 Foam-PCM Interface

This work uses high-resolution infrared microscopy enabling direct observation of the temperature distribution across the interface between the foam and PCM. For this analysis, one foam sample (the 10 PPI) was chosen and the interface temperature distribution was evaluated throughout the solidification process. Figure 4.24 highlights the region selected for analysis which consists of a foam element sandwiched between two PCM pockets. The temperature was plotted at selected time intervals to explain what is going on at the interface level. As we can see from the Figure 4.25 (panels (b)-(i)) the temperature in foam is lower than the PCM by several degrees. The foam can quickly dissipate heat to the aluminum pipe and cooling fluid by lowering the temperature foam temperature fairly uniformly, but the PCM temperature lags behind the foam temperature due to the low conductivity and melting behavior. Further, there may be an interface resistance contributing to the temperature lag, but additional higher resolution tests are required to validate that hypothesis. Figure 4.26 shows the temperature distribution at different time intervals for the 10PPI foam sample across a selected region of study, which included two PCM zones and

one foam filament sandwiched in between.

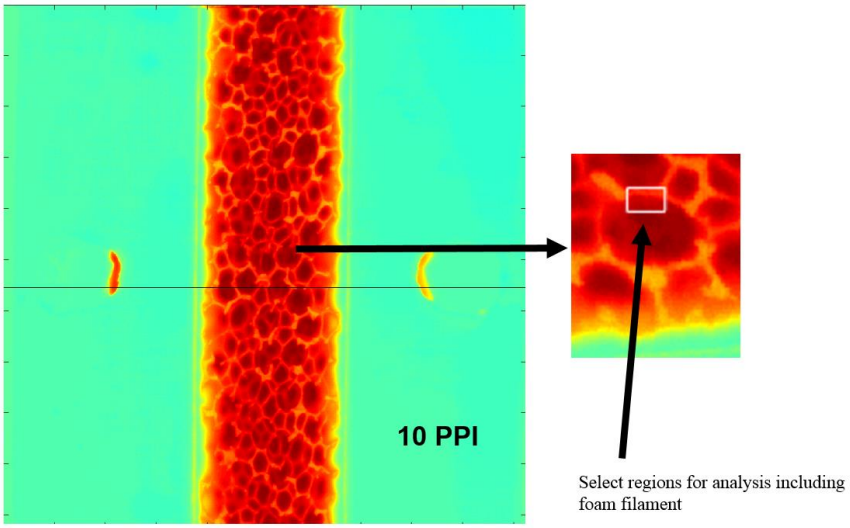

Figure 4.24 Thermal image of the 10 PPI foam. The inset shows a region selected for analysis including a metal filament and the PCM pore. The selected region consists of a metal foam filament sandwiched between two PCM pockets

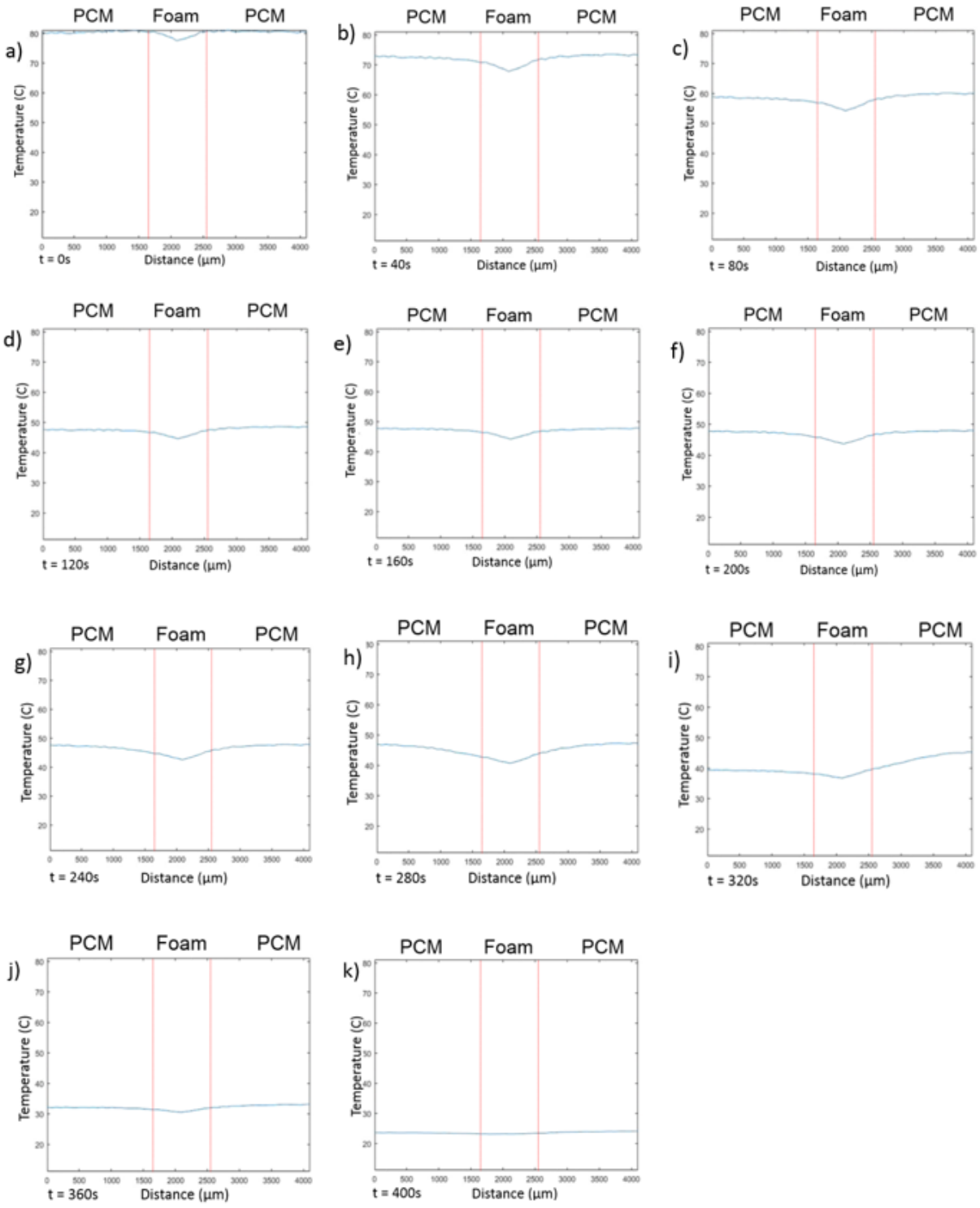

Figure 4.25 Temperature evolution across the Foam-PCM Interface. Note that the temperature distribution is similar from 80-280 s (panels (c-h)) because phase change is occurring. The foam temperature is always lower than the PCM during solidification

4.6. Conclusions:

The heat spreading capability of foams shortens the phase change response time, which will ultimately benefit the thermal storage industry, as response time is an important design parameter for any heat recover/thermal storage system. The foams convert the phase change into a more localized process within each pore, rather than throughout the whole PCM chamber. This is possible because of the network of metal filaments throughout foams, which breaks the PCM sample into smaller chunks that can undergo phase change much more rapidly as compared to a bulk PCM sample.

Foams enhance the overall thermal conductivity of composite system, which also helps in reducing the phase change response time. The foams used in this experiment are around 92% porous, which translates to an effective thermal conductivity of 3.43 W/m/K and is 13 times greater than PCM alone. There is also slight reduction in the solidification time of foams with decreasing pore size (increasing PPI).

The solidification time reduced by a factor of 2.8 or 53%. Thus, the reduced response time is crucial to reset the system, which boosts the overall efficiency of the thermal storage system. The effect of the pore size (PPI) on the solidification times was not significant compared to the improvement of adding any foam. Further tests are needed to see how porosity effects phase change by quantifying the convection effects and interface propagation in the sample.

Further, high-resolution infrared thermal imaging observed the interface between the foam and PCM throughout the solidification process, observing that the metal is always cooler than the PCM. More work is needed to identify if thermal resistances are important in these systems.

CHAPTER 5. CONCLUSIONS

The project provided insight into the dynamics of phase change materials embedded in high conductivity metal foams. First, the melting and solidification behavior was observed in mm-scale isolated holes that somewhat represent pores in the foams. The melt/solidification front propagation and the radial temperature distribution profiles provided key information on pore level phase change dynamics. Then, the melting and solidification behavior was directly observed for aluminum foams of different pore sizes finding a significant improvement in the response time and temperature uniformity with the foams. The factor of 3 improvement in response times, demonstrate that foams are useful for thermal energy storage systems. The PCM-foam interface was investigated to understand the heat flow across it, which sheds light on the thermal interaction between the foam (heat spreader) and the PCM (thermal storage) components. The present analysis is a launching point for future thermal storage studies based on Foam-PCM systems. Future work should include an analytical study into the thermal transport at the pore level, and improved quantification the fluid dynamics of the flow loop and convection effects within the molten phase change materials. More pore sizes will be considered for analysis to better quantify pore diameter on phase change dynamics. Cycling will be carried out for melting/solidification to see how hysteresis effects heat spreading. The foam-PCM interaction will be better quantified by computing the interfacial contact conductance.

REFERENCES

[1] "ENERGY STORAGE: THE BASICS" Retrieved from *http://www.low-carbonscotland.scot/wp-content/uploads/2016/02/Energy_Storage-The_Basics-Scottish_Renewables.pdf*, 2015

[2] "The end of fossil Fuels", Retrieved from *https://www.ecotricity.co.uk/our-green-energy/energy-independence/the-end-of-fossil-fuels*

[3] L Doman (World Energy consumption by 20140". Retrieved from *https://www.eia.gov/todayinenergy/detail.php?id=32912*, 2015.

[4] M Kita, "The types of Energy storage systems". Retrieved from *http://acheng.us/types-of-thermal-energy-storage-systems/*, 2017.

[5] L Smith *et al.*. "25 kW Low-Temperature Sterling Engine for Heat Recovery, Solar, and Biomass Applications", *International Statistical Ecology Conference, Seattle*, 2016.

[6] Arju,"Phase Change Material". Retrieved from *https://steemit.com/science/@arju/phase-change-material-pcm-steemiteduction-1*, 2017.

[7] B Styles, "US Patent No 960,590,6B2, South Field, MI, *DENSO INTERNATIONAL AMERICA, INC,* 2017.

[8] E Elnajjr, "Using PCM embedded in building material for thermal management: Performance assessment study", *Energy and Buildings*, vol 151, pp 28-34, 2017

[9] V K Dwivedi *et al.*,"Importance of phase change material (PCM) in solar thermal applications: A review", *International Conference on Emerging Trends in Electrical Electronics & Sustainable Energy Systems (ICETEESES)*, 2016.

[10] C. Gao *et al.* ,"Personal cooling with phase change materials to improve thermal comfort from a heat wave perspective", *Indoor Air, John Wiley and Sons*, vol 22,pp 523-530, 2012

[11] A.S. Fleischer, "Thermal Energy Storage Using Phase Change Materials", *Springer Briefs in Thermal Engineering and Applied Science*, pp 29-32, 2015.

[12] "Energy Storage: Phase change materials for thermal energy storage", Retrieved from *http://www.climatetechwiki.org/technology/jiqweb-pcm-0*.

[13] A Albury, “Why Thermal conductivity matters”. Retrieved from *http://www.puretemp.com/stories/why-thermal-conductivity-matters*, 2016.

[14], L F Cabeza ,"Thermal Energy Storage, in Comprehensive Renewable Energy", A. Sayigh, Editor, and Elsevier: Oxford. pp 211-253, 2012.

[15] "Which Metal conducts heat best?"), Retrieved from *https://www.metalsupermarkets.com/which-metals-conduct-heat-best/*.2016.

[16] A Arshad *et al.*,"Thermal performance of phase change material (PCM) based pin-finned heat sinks for electronics devices: Effect of pin thickness and PCM volume fraction", *Applied Thermal Engineering*, vol 112, pp 143-155, 2017.

[17] Yang *et al*, “Finned Heat pipe assisted low melting point PCM Heat sink against extremely high power thermal shock”, *Energy Conversion and Management*, vol 180, pp 467-476, 2018.

[18].Pincemin et al ,"Highly conductive composites made of phase change materials and graphite for thermal storage", *Solar Energy Materials & Solar Cells*, vol 92,pp 602-613 ,2008.

[19] Goli *et al*, “Graphene enhanced hybrid phase change materials for thermal management of Li-Ion batteries,”, Journal of Power Sources, vol 248, pp 37-43, 2014.

[20]“Technical Products Function Sheet”, Retrieved from fxi.com/assests/pdf/FS_MEC4.pdf

[21] A F Mustaffar,"Irregular aluminum foam and phase change material composite in transient thermal management", PhD Thesis, School of Chemical Engineering and Advanced Materials, *New Castle University*, New Castle,UK, 2016.

[22] H Ji *et al.*,"Enhanced thermal conductivity of phase change materials with ultrathin-graphite foams for thermal energy storage", *Energy & Environmental Science*, Issue 3,no 7,pp 1185-1192, 2014.

[23] A. Fleischer, “Energy storage applications”, in *Thermal Energy Storage Using Phase Change Materials*, Heidelberg: Springer Cham, , pp.7-31, 2015

[24] D.J. Malan *et al.*, “Solar thermal energy storage in power generation using phase change material with heat pipes and fins to enhance heat transfer”, *Energy Procedia*, vol. 69, pp:925-936, 2015.

[25] Y. Ganatra and A. Marconnet, “Passive Thermal Management Using Phase Change Materials: Experimental Evaluation of Thermal Resistances”, *International Technical*

[26] *Conference and Exhibition on Packaging and Integration of Electronic and Photonic Microsystems (InterPACK)*, San Francisco, CA, 2015.

[27] C Gao *et al.*, "Personalized cooling with phase change materials in very hot environment", *Fourth International Conference on Human Environment System*, 2011.

[28] Dukhan *et al.*, "An improved PCM heat storage technology utilizing metal foams, *12th IEEE Intersociety Conference on Thermal and Thermomechanical Phenomena in Electronic Systems*, 2-5 June, Las Vegas, Nevada. 2010.

[29] Hu *et al.*, "Experimental Study on the Cooling Charge and Discharge Characteristics of a PCM Based Fin–Tube Thermal Energy Storage Exchanger*", Procedia Engineering*, vol. 2015, pp: 3088-3095, 2017.

[30] M. N. A. Howlader, M. S. Uddin, and H. J. Zhu, "Encapsulated Phase Change Materials for Thermal Energy Storage: Experiments and Simulation", *International Journal of Energy Research*, vol. 26, pp. 159-171, 2002.

[31] D. Sun, S. R. Annapragada, and S.V. Garimella, "Experimental and Numerical Study of Melting of Particle-Laden Materials in a Cylinder", *International Journal of Heat and Mass Transfer*, vol. 52, pp. 2966-2978, 2009.

[32] Hlimi *et al.*, "Melting Inside a Horizontal Cylindrical Capsule", *Case Studies in Thermal Engineering*, vol. 8, pp. 359-369, 2016.

[33] N. S. Dhaidan and J.M. Khodadadi, "Melting and convection of phase change materials in different shape containers: A review", *Renewable and Sustainable Energy Reviews*, vol. 43, pp: 449-477, 2015.

[34] B J. Jones *et al.*," Experimental and numerical study of melting in a cylinder*", International Journal of Heat and Mass Transfer*, vol. 49, pp: 2724-2738, 2006.

[35] H. Shmueli *et al.*," Melting in a vertical cylindrical tube: Numerical investigation and comparison with experiments", *International Journal of Heat and Mass Transfer*, vol. 53, pp: 4082-4091, 2010.

[36] Y. K. Wu and M. Lacroix, "Melting of a PCM inside a vertical cylindrical capsule*", International Journal for Numerical Methods in Fluids*, vol. 20, pp: 559-572, 1995.

[37] M. D. Muhammad *et al.*," Validation of a CFD Melting and Solidification Model for Phase Change in Vertical Cylinders", *Numerical Heat Transfer, Part A: Applications*, vol. 68, issue 5, pp: 501-511, 2015.

[38] E. M. Sparrow and J. A. Broadbent, “Inward Melting in a Vertical Tube Which Allows Free Expansion of the Phase-Change Medium”, *ASME Journal of Heat Transfer*, vol. 104, No. 2, pp: 309-315, 2009.

[39] Entropy Solutions, “Pure Temp 42 Technical Data Sheet”, 2014. Available*: http://www.puretemp.com/stories/puretemp-42-td*, [Accessed: Oct 15 2017]

[40] H Zheng *et al.*. "Numerical and Experimental Studies on the Heat Transfer Performance of Copper Foam Filled with Paraffin", *Energies, MPDI*, vol 10, Issue 7, pp 902-915, 2017.

[41] N Trifale *et al.*,"Thermal and Mechanical Modeling of Metal Foams for Thermal Interface Application", *ASME Journal of Heat Transfer*, vol 138, Issue 7, pp 072801-072801-12, 2016.

[42] G R Jackson *et al.*,"Simulation of thermal storage in PCM-impregnated porous foams with a pore-scale sub model*", 11th AIAA/ASME Joint Thermophysics and Heat Transfer Conference, AIAA AVIATION Forum, (AIAA 2014-3122)*, 2015.

[43] T Kim *et al.*,"Heat transfer analysis of a latent heat thermal energy storage system using graphite foam for concentrated solar power", *Solar Energy*, vol 103, pp 438-447, 2014.

[44] X Huang *et al.*, "Thermal properties and thermal conductivity enhancement of composite phase change materials using myristyl alcohol/metal foam for solar thermal storage”, *Solar Energy Materials and Solar Cells*,vol 170, pp 68-76, 2017.

[45] D Singh *et al.* ,"Analysis of a graphite foam–NaCl latent heat storage system for supercritical CO2 power cycles for concentrated solar power”, *Solar Energy*, Vol 118, pp 232-242, 2015.

VITA

Prahlad Kulkarni is a Graduate Student at Purdue University since Fall 2016. He has been working on the Foam – PCM thermal interaction for thermal energy storage since fall 2017. Prior to that, he worked on another project: Passive thermal management using phase change materials (Affiliated to CTRC (Cooling Technologies Research Center)). He graduated with Bachelors in Mechanical Engineering from R V College of Engineering in Bangalore, India.